2022

A Predictive Modeling Approach to Counter Failures in Heat Seal Process Verification Methods

Charles Albanese
n00034207@unf.edu

A Predictive Modeling Approach to Counter Failures in Heat Seal Process Verification Methods

by

Charles Gerard Albanese

A Thesis submitted to The College of Computing Engineering and Construction

in partial fulfillment of the requirements for the degree of

Master of Science in Electrical Engineering

UNIVERSITY OF NORTH FLORIDA

COLLEGE OF COMPUTING, ENGINEERING & CONSTRUCTION

August 2022

ACKNOWLEDGMENTS

I would like to thank the thesis committee members, Dr. O Patrick Kreidl, my supervising professor, for his continuous direction and encouragement during this process, Dr. John Nuszkowski for his help and assistance in the realm of thermodynamics, and Dr. Alan Harris for his feedback and advice.

TABLE OF CONTENTS

Page

CHAPTER 1: INTRODUCTION 1

CHAPTER 2: BACKGROUND AND LITERATURE REVIEW 4

2.1 Heat Seal Process 4

2.2 Heat Seal Verification Test Methods 5

2.3 Study Using a Constant Cycle Time for the Heat Seal Process 6

2.4 Study on the Effects of Platen Temperature and Dwell Time for The Heat Seal Process 7

2.5 Study on The Heat Seal Process for Various Materials 8

2.6 Study on the of Finite Difference Methods Applied to a Heat Seal Process 10

CHAPTER 3: HEAT SEAL MODEL 11

3.1 The Package 11

3.2 First Principal Equations 12

3.3 State Space Model 13

3.4 Heat Seal Model Assumptions 16

3.4.1 Pressure 17

3.4.2 Heater Block 17

3.4.3 Contact Area 18

3.4.4 Material 19

3.5 Simulation Results Open Loop 20

CHAPTER 4: POLYNOMIAL / TRANSFER FUNCTION MODEL SIMPLIFICATION 22

4.1 Sample Size 22

4.2 MATLAB System ID 23

4.3 ANOVA 26

CHAPTER 5: STATE SPACE MODEL WITH FEEDBACK 33

5.1 Controllability and Observability 33

5.2 Model Stability 35

5.3 Linear Quadratic Regulator (LQR) 38

5.4 Linear Quadratic Regulator (LQR) Stability 39

5.5 Linear Quadratic Regulator (LQR) Performance and Effort 40

5.6 Linear Quadratic Tracker (LQT) 41

5.7 Simulation Experiments 42

CHAPTER 6: CONCLUSION 47

CHAPTER 7: FUTURE WORK 49

CHAPTER 8: BIBLIOGRAPHY 50

CHAPTER 9: APPENDIX 60

9.1 MATLAB Code 60

LIST OF TABLES

Table 1 System Inputs, Outputs, and States 15

Table 2 MATLAB Variables Names 15

Table 3 System ID *arx* Best Fits 26

LIST OF FIGURES

Figure 1 Pharmaceutical Packages (courtesy of Rockwell Automation Inc, 2022) 1

Figure 2 Existing Process, Open Loop, Closed Loop (Intellegens, 2022) (NAJARZADEH, 2022) (Toolbox, 2022) (Wang, 2022) (Grab, 2022) (Corporate Finance Institute (n, 2022)..... 3

Figure 3 Heat Seal Process (Wiley, 2021)..... 5

Figure 4 Determination of the Inflection Point (Aithani, Lockhart, Auras, & Tanprasert, 2006) . 9

Figure 5 Dairy Cup Sealing Layers Block Diagram (Gunter Schubert) 12

Figure 6 State Space Model Matrix or Vectors (ShareTechNote, n.d.) 13

Figure 7 State Space Models – Feed Forward (Toolbox, 2022)..... 14

Figure 8 State Space Models – No Feed Forward (Toolbox, 2022)..... 14

Figure 9 Pressure Multiple Levels (Clark, 2022) 17

Figure 10 Heater PID Control (PID'S, 2015) (Mohammed)..... 18

Figure 11 Heat Conduction through Contacting Points (Mantelli & Yovanovicht, 2022) 19

Figure 12 Heat Seal – State Space – Open Loop..... 21

Figure 13 ± 5% Model Data Set..... 25

Figure 14 Best Fit Plots – S1 – *arx* and Transfer Function Models..... 26

Figure 15 Best Fit Plots – S2 – *arx* and Transfer Function Models..... 27

Figure 16 Best Fit Plots – S3 – *arx* and Transfer Function Models..... 27

Figure 17 Best Fit Plots – S4 – *arx* and Transfer Function Models..... 28

Figure 18 Best Fit Plots – S5 – *arx* and Transfer Function Models..... 28

Figure 19 Best Fit Plots – S6 – *arx* and Transfer Function Models..... 29

Figure 20 Best Fit Plots – S7 – *arx* and Transfer Function Models..... 29

Figure 21 Best Fit Plots – S8 – *arx* and Transfer Function Models 30

Figure 22 Anderson-Darling Test Logical and P Value Results 31

Figure 23 ANOVA Max, 75%-ile, median, 25%-ile and Min for Each Model. 32

Figure 24 Critical States / System Outputs 34

Figure 25 Common Bicycle (Bikes, 2022) 35

Figure 26 Linear Stability Analysis (Mossa, 2021, 13, 502–532) 36

Figure 27 Stability Unit Circle (Wang, 2022) 37

Figure 28 System ID Unit Circle Pole / Zero Plot 38

Figure 29 Pole Placement and LQR Control (Douglas, State Space, Part 4: What Is LQR Control, 2022) 39

Figure 30 LQR State Space Model (Toolbox, 2022) 40

Figure 31 Performance [Q] and Effort [R] (Douglas, State Space, Part 4: What Is LQR Control, 2022) 40

Figure 32 Dinner Party Performance [Q] and Effort [R] *Figure 32* (MOM, 2022) (Dishwashers, 2022) (News, 2022) (PJ, 2022) (Pinterest, 2022) 41

Figure 33 Good Profile 43

Figure 34 Bad Profile Below 44

Figure 35 Bad Profile Above 44

Figure 36 Performance [Q] and Effort [R] 45

Figure 37 LQTY Corrected Profile Below 46

Figure 38 LQTY Corrected Profile Above 46

ABSTRACT

Most products sold today are packaged in a protective shell that involves the design of a box or wrapper. A subset of such products also adds a second layer of protection via sterilization. For both sterilized and non-sterilized products, a procedure referred to as the heat seal process creates the protective barrier from outside influence. For sterilized products, the American Society for Testing and Materials provides standards to test or verify seal strength, and this verification is normally accomplished by using a process called a Design of Experiments (DOE). The DOE method makes systematic use of powerful data collection and analysis tools, however, it also takes considerable time, capital, and resources to implement and verify. Moreover, when changes to the system or materials are necessary, the needed re-verification of the process compounds the effort needed to complete a subsequent DOE analysis.

The objective of this thesis is to demonstrate the use of control-theoretic modeling and prediction algorithms to reduce the burden of DOE methods for heat-seal processes. Specifically, assuming the DOE analysis can collect data with sufficient instrumentation, we illustrate a two-pronged approach that employs (i) model identification from data to discern between success/failure of a heat-seal process and (ii) model-based feedback control to determine process reconfigurations towards failure recovery. Simulation experiments are presented that mimic the advent of heat-seal failures due to a new foil material and employ our approach to recover successful seals through minimal adjustments to the heater's temperature profile. The extent to which the approach can apply to other process failure scenarios, different configurable inputs (e.g., seal pressure) or under non-ideal instrumentation assumptions is cited as future work.

CHAPTER 1: INTRODUCTION

Most products sold today are packaged and shielded from outside influence by the creation of a box or wrapper that contains the product. The container may provide brand names, directions of use or safety instructions, while also adding a layer that further shields the product from environmental influences. A subset of products sold require the additional layer to keep the product sterilized; for example, this layer may serve to avoid the risks of microbial degradation or infection occurring during their use. Examples of such products include drug delivery systems and medical devices as seen in *Figure* 1 (Rockwell Automation, Inc., 2022).

Figure 1 Pharmaceutical Packages (courtesy of Rockwell Automation Inc, 2022)

To create such protective barriers, a manufacturing system will typically use a heat-sealing process. Any such process must be verified or qualified using the Design of Experiments (DOE) method (Moresteam, 2022) . DOE methods are based on the gathering empirical data from secondary parameters or variables because it is often impossible or cost-prohibitive to instrument all areas of interest due to the physical design of the package and/or environmental factors of the system. A sensor placed within the sealing area, for example, could inhibit or diminish the seal integrity of the package itself. Additionally, seals are usually formed through heat bursts under high-pressure, which upon contact could destroy the sensor before useful data is acquired. Finally,

in practice, DOE methods cost a manufacturing company time, money and resources not just prior to product launch but throughout the product's lifetime. This is because the evolving system and/or varying materials may push the system to operate outside boundaries set during a previous DOE, which could lead to an unverified state until the process is revalidated.

One of the objectives of this project was to review past experiments, to be conscious of previous practices, and to perhaps identify gaps and or ways to remodel existing methods. A common theme of all the reviewed literature was to quantify and understand the thermochemistry, chemical reactions, and phase changes between layers and materials during the sealing process. Coincidently understanding this is essential to overcome the drawbacks of using the DOE process as a qualification method.

The method suggested here is the design and simulation of a state-space mathematical model using first-principle physics laws combined with material properties to expose and evaluate the interactions between layers would overcome the disparity within the DOE process.

The first iteration of the model will simulate a system configured in an open loop mode. This operating mode is typical of how the majority of heat seal systems are designed, i.e., a sensor in the heater control loop that controls the temperature of the heating die but no sensor that measures temperatures for the medium package interface layers. Verifying this model would be a major step forward in reducing the DOE time and resources and there would be a better realization on how changes to the system and or materials will affect the states of the system. Figure 2 below shows the existing DOE process in the blue box and the first method proposed in this paper in the dotted orange box.

Data from the open loop system will then be used within the MATLAB system ID tool to generate polynomial and transfer function models. Polynomial and transfer function models will be used to simply the system and the be inspected for stability, controllability, and observability. This is shown in Figure 2 within the dotted blue box.

The second iteration or possible future state of the heat seal model will use the results from the polynomial and transfer function analysis to be incorporated into closed loop design that is focused on the medium package interface by using a subsequently developed sensor, a mathematical estimator or observer that will provide the state feedback that will be used within modern control techniques. The intent of this model is to provide near real time control that can be used during nominal material variations, intended changes to sealing materials, or modifications to the system. This model, with an advanced sensor or a mathematical estimation as the input would remove the need to run a DOE process.

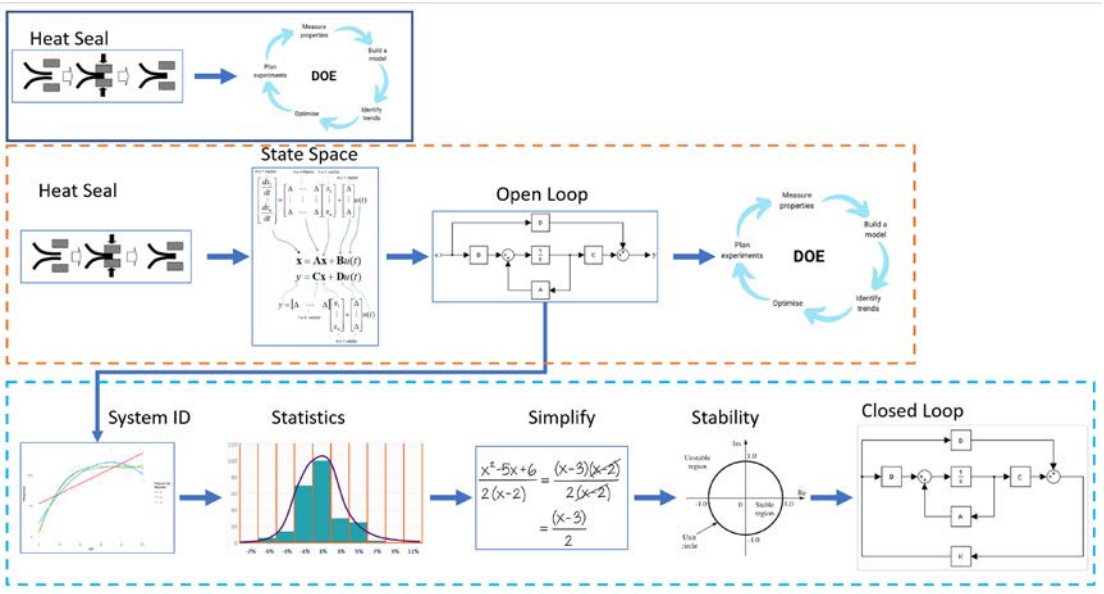

Figure 2 Existing Process, Open Loop, Closed Loop (Intellegens, 2022) (NAJARZADEH, 2022) (Toolbox, 2022) (Wang, 2022) (Grab, 2022) (Corporate Finance Institute (n, 2022)

CHAPTER 2: BACKGROUND AND LITERATURE REVIEW

Many previous heat seal experiments or studies have been performed and the focus has been to understand the effects or influences either combined or individually that the system inputs to include packaging materials, system materials, time, temperature, and pressure have on the system outputs, such as the strength, quality, and reliability of the resulting heat seal.

2.1 Heat Seal Process

A basic four-step overview of the heat seal process is shown in Figure 2 (Wiley, 2021). The initial state assumes the two layers are separated. The *print* layer is where information about the contents of the package are printed, which may include product name, direction of use, manufacture and other data depending on what regulatory requirements are necessary. The *barrier* is the layer that isolates the contents of the package from the outside world. The *sealant* layer and the *adhesive* layer serve to bond the barrier and the package together when subjected to heat. Established system designs of the heat seal process involve first selecting material parameters within these layers. The dynamics expressed within the design become relevant within steps two and three in *Figure 3*, which is when the applied heat source along with the parameters of time and pressure interact with the intended layered materials. In practice, it is often difficult to obtain confidence and accuracy of the transient states in steps two and three and the predicted terminal state in step four. Thus, the design is verified via Design-of-Experiments (DOE) using secondary

process parameters, temperature, time, pressure, and package integrity testing against the terminal state of step four.

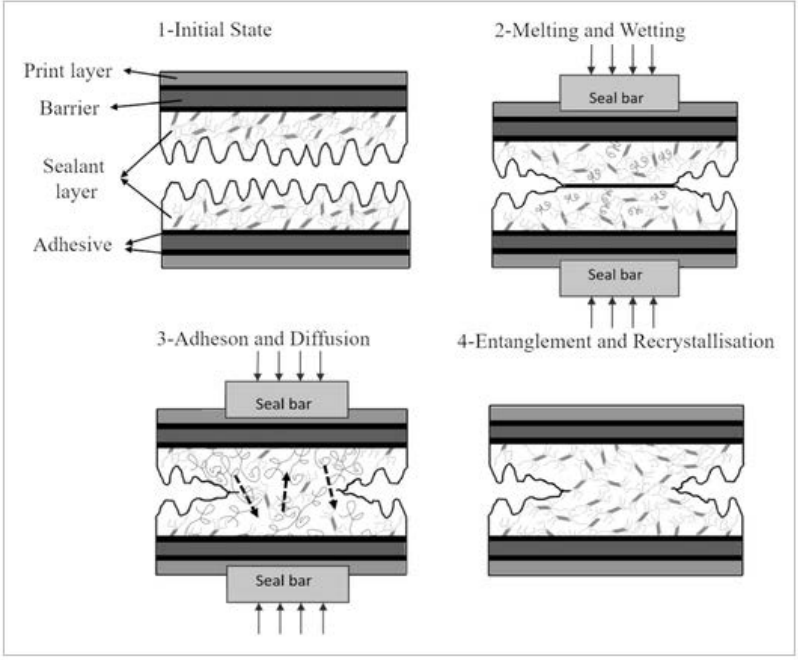

Figure 3 Heat Seal Process (Wiley, 2021)

2.2 Heat Seal Verification Test Methods

The Design-of-Experiments (DOE) technique ensures that the package design along with the process parameters, time, temperature, and pressure setpoints meet or exceed the package integrity testing standard defined by the American Society of Testing and Materials (ASTM). The (ASTM) sets the standards for test methods used to determine the seal strength of flexible barrier materials. ASTM F88 is a test for seal strength and the units are measured in pascal (Pa) or Newtons per square meter (N/m^2); with this measurement, there exist standards accepted by industry to determine the tensile strength of the bonded materials. (Mecmesin, 2022). ASTM

F3039 is another standard that covers how to determine the presence of gaps or macroscopic holes that the tensile strength test may not reveal; specifically, ASTM F3039 provides a standard to detect “leaks in nonporous packaging or flexible barrier materials by submerging the packages into a liquid dye.” (American National Standards Institute, 2022) It is worth noting that neither ASTM F88 or F3039 standardize the choice of material properties or parameters used in a design. In other words, the combination of materials selected by the package designer will be a major factor in determining if the package will ultimately pass the ASTM testing. This gap between the ASTM standards and the lack of real-world in relation to transient states and the predicted terminal state is why current practices continue to depend on burdensome DOE verification, and the key premise motivating this thesis, namely, to demonstrate the use of control-theoretic modeling and prediction algorithms to reduce the burden of DOE methods for heat-seal processes.

2.3 Study Using a Constant Cycle Time for the Heat Seal Process

The knowledge of how many parts per minute a machine can produce affects sales, capital expenditures, budgets, infrastructure decisions, personal, investment, and many other business categories for any manufacturer. A machine that has a constant cycle time will allow a predicted throughput and can be critical in business models and monetary decisions.

In the publication The Effect of Heat-Sealing Temperature on the Properties of OPP/CPP Heat Seal. I. Mechanical Properties (Tsujii Tetsuya, Ishiaku, Mizoguchi, & Hamada, 2004) the experiment emphasized keeping the heat-sealing time at a constant while changing the temperatures. The study was based on the premise of understanding the material integrity and morphology of oriented polypropylene (OPP) cast polypropylene (CPP) laminated films used a sealing process.

The results show the effect temperature has on the seal peel strength and the data showed when the temperatures exceeded a certain value, the package strength value reached a maximum and strength remained relatively constant even as temperature increased on a linear scale.

This study has shown that if the heat seal process must have a constant cycle time while using the materials listed in the publication, the temperature can be modified to achieve a certain seal strength criterion. It also shows that the material combination used in this study has a maximum seal strength; it can produce, if the desired seal straight exceeds what this material can achieve, a new combination of materials must be selected.

2.4 Study on the Effects of Platen Temperature and Dwell Time for The Heat Seal Process

Heat Sealing of linear low-density polyethylene (LLDPE): Relationships to Melting and Interdiffusion studied "the effect of heat-sealing variables (platen temperature and dwell time) on seal strength using the material of LLDPE" (Mueller, Capaccio, Hiltner, & Baer, 1998).

This source used the ASTM F88 method in a T-peel configuration to determine peel strength. The peel strength is determined by pulling the sample at a constant speed, dividing the average measured force to separate two fused heat-seal films by the unit width of the films (ADMET, 1994 - 2021).

The results are material dependent for LLDPE, examining the sealing time curve at $\approx 110^{O}C$ a weak seal would be produced even if the time was extended to 10K seconds, alternatively at $125^{O}C$ at 1 second the seal strength 8 times higher. When used in conjunction, temperature and time can influence the desired strength for LLDPE. Every manufacturing process is unique and when considering a design that needs a short cycle time using LLDPE the results show an inverse correlation between temperature and time related to peel strength.

This study discussed in detail the underlying material properties involved in achieving a strong seal. The following encompasses the main motivation for this thesis. “To use the empirical approach to understand the relationships between melting and interdiffusion does not consider types of melted chains (molecular weight, branch content, or comonomer content) thus there is a lack of understanding of what effect the thermal process is having within the seal area” (Mueller, Capaccio, Hiltner, & Baer, 1998).

2.5 Study on The Heat Seal Process for Various Materials

A different emphasis was used by Heat Sealing Measurement by an Innovative Technique (Aithani, Lockhart, Auras, & Tanprasert, 2006) that focused on the seal strength and how the seal strength was affected by using different sealing materials to include low density polyethylene (LDPE), high-density polyethylene (HDPE), linear low-density polyethylene (LLDPE) and cast polypropylene (CPP).

This approach was concentrated around a mathematically derived inflection point by creating a technique called “methods for measuring temperature of melting surface (MTMS)” (Aithani, Lockhart, Auras, & Tanprasert, 2006). The logic is if “there is a change in the heat conductivity near the inflection point, which results in a change in heat flow rate and hence an inflection point (a point on the time–temperature profile where the second derivative changes sign from – to +: the temperature at the inflection point is called the fusion temperature” (Aithani, Lockhart, Auras, & Tanprasert, 2006). The deflection points or the second derivative are shown in *Figure 4* (Aithani, Lockhart, Auras, & Tanprasert, 2006).

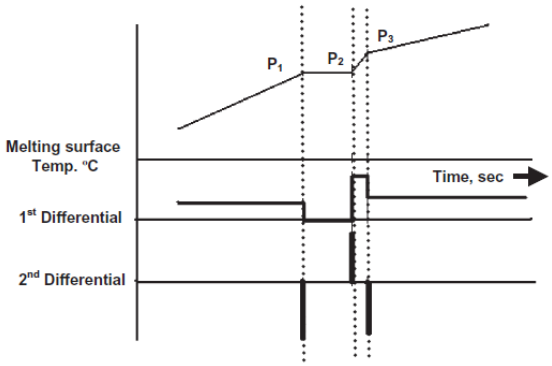

Figure 4 Determination of the Inflection Point (Aithani, Lockhart, Auras, & Tanprasert, 2006)

The instrument used to measure the inflection point of the listed material was a Differential Scanning Calorimeter (DSC); "this instrument measures the temperatures and heat flows associated with thermal transitions in a material" (Instruments, 2022). These instruments are used in labs and for quality product sampling but a big caveat about the DSC process is that it is destructive, i.e., the product tested within this instrument will not be able to be used for its design intent.

The DSC, MTMS, and inflection point results were provided for each material tested and the results show that materials tested have an individual film melting temperature, measuring temperature of melting surface (MTMS) or inflection point, which would be expected so each film will have a separate heat-sealing profile.

The findings also show how pressure has limited influence. "An experiment was conducted to observe the effect of sealing pressure on the inflection point of the polymer film. Changes in sealing pressure within the range of pressure tested did not affect the inflection point. This indicates the limited effect of pressure on seal strength, and it should be sufficient to bring the sealing films into intimate contact, as studied by, as studied by (Theller, 1989) and (Meka & Stehling, 1994)."

2.6 Study on the of Finite Difference Methods Applied to a Heat Seal Process

Heat Sealing Fundamentals (Heat Sealing Fundamentals, 2015) used finite difference methods to develop mathematical models. The methodology used was to create a three-dimensional heat diffusion equation with no energy generation and then derive the finite difference equations. This method was to determine the final temperature that can be related to seal strength. The researchers stated that “The material combinations used in specific packaging applications and their interactions with the thermal and physical conditions of the process will dictate the final quality of the seal. To optimize these conditions for selected materials, comprehensive knowledge of the process itself is needed in combination with supporting computational and experimental tools” (Heat Sealing Fundamentals, 2015).

A similar and alternate approach, proposed here, would use first principal equations that describe thermal losses and the conservation of energy within a controlled volume that are applied to a state space mathematical model to simulate and predict the systems behavior. This effort can analyze and predict how changes to the system inputs, or the system material parameters will affect the process. The state space model has the capability to control and observe the system and contains the ability to correct the process. The system parameters can be configured for any design configuration and can show the effects on the system states.

CHAPTER 3: HEAT SEAL MODEL

The first objective for model design was to search for random packages where certain attributes could be used without infringing on intellectual properties or trade secrets. The objective of this chapter is to define an open-loop state space model that is well-suited for heat-seal simulations. Details on the first principal equations, materials and parameters that would be used in the mathematical architecture of the state space model will be discussed along with the model assumptions used during simulation.

3.1 The Package

The package selected for this research was a layered representation of a simple dairy cup as shown in *Figure 5* (Gunter Schubert). The cup was chosen due to the fact it has real world materials used in a sealing process. No other parameters were used from this source such as temperature, physical dimensions because this study was a hot-tack package integrity test that measures good seal integrity indirectly.

The left side shows the fictious system in layers and where the temperature measurement will be simulated to include the heater, medium package interface and the package itself. The medium package interface contains three layers. The right side shows the materials used in this model.

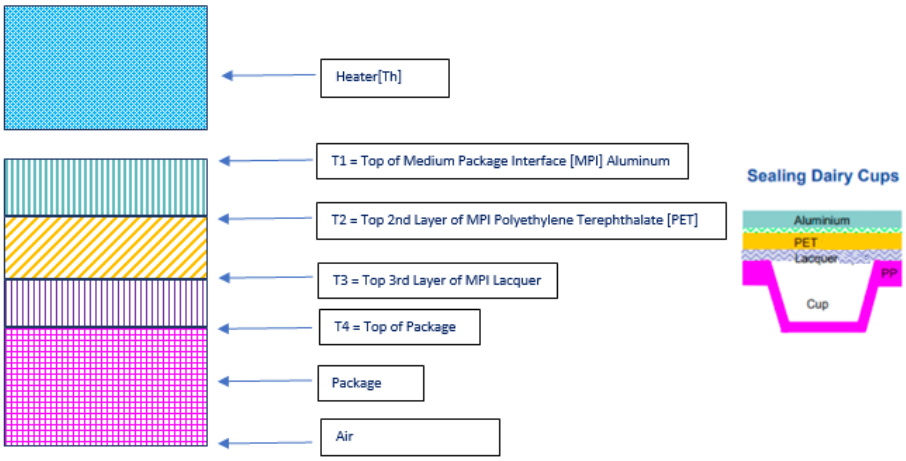

Figure 5 Dairy Cup Sealing Layers Block Diagram (Gunter Schubert)

3.2 First Principal Equations

The model construction used the first principal equations for heat transfer which includes Fourier's law of heat conduction for losses between layers or thermal resistance and the first Law of Thermodynamics for a Closed Loop System which includes thermal capacitance.

Fourier's law of heat conduction states "it has been experimentally observed that the rate of heat conduction through a layer is proportional to the temperature difference across the layer and the heat transfer area, but it is inversely proportional to the thickness of the layer" (Bahrami, n.d.). Denoting by dT/dx the temperature gradient, which is the slope of the temperature curve (the rate of change of temperature T with length x) the formula is.

$$Q = -k_d A \frac{dT}{dx} \qquad (1)$$

For steady conduction through a constant area plane wall, heat conduction can be stated in (2) where Q is watts, a is cross-sectional surface area; k_d is thermal conductivity; L is meters, and T is degrees Celsius.

$$Q = -k_d A \frac{dT}{dx} = \frac{a\, k_d\, (T_1 - T_2)}{L} \quad (2)$$

Finally, the first Law of Thermodynamics for a Close Loop System, or the thermal capacitance without reference to work at a constant volume, is shown in (3) (Lienhard & Lienhard, 2019) where m_v is mass, c_v is specific heat, and Q is Watts.

$$m_v * c_v * \frac{dT}{dt} = Qin - Qout \quad (3)$$

3.3 State Space Model

As described by MATLAB (MathWorks, 1994-2022), the state-space model object can represent single input single output (SISO) or multiple inputs multiple outputs (MIMO) in continuous time or discrete time. The open loop heat seal model will be a MIMO model in the form of $states = (x) \in R^n$, $inputs = (u) \in R^m$, $outputs\ (y) \in R^p$ as shown in *Figure 6* (ShareTechNote, n.d.).

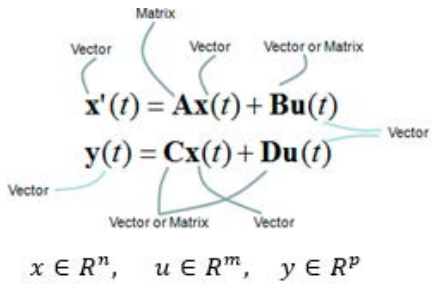

Figure 6 State Space Model Matrix or Vectors (ShareTechNote, n.d.)

Figure 7 (Toolbox, 2022) shows the state space model in a block diagram illustration. The A is the system matrix, B is the input matrix, C is the output matrix, and D is the feed-forward matrix as described by state space models (Toolbox, 2022).

The heat seal model did not use the D matrix (i.e., assumes D is the zero matrix). An example D matrix is cruise control on a car; the car approaches a hill; the system uses an instrument to measure the slope of the hill, a change in slope, the system accelerates or decelerates prior to reaching the hill to keep a steady speed (Engineering). An example without feed forward is shown in *Figure 8*

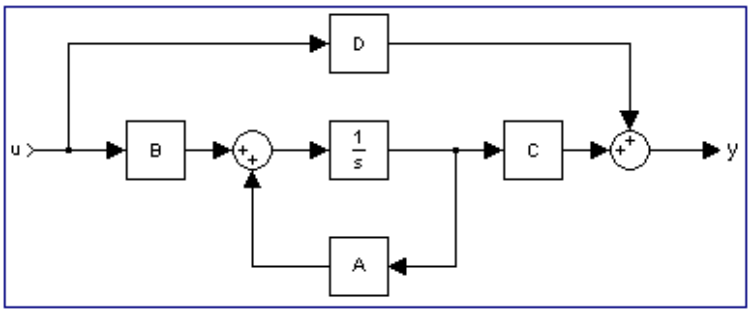

Figure 7 State Space Models – Feed Forward (Toolbox, 2022)

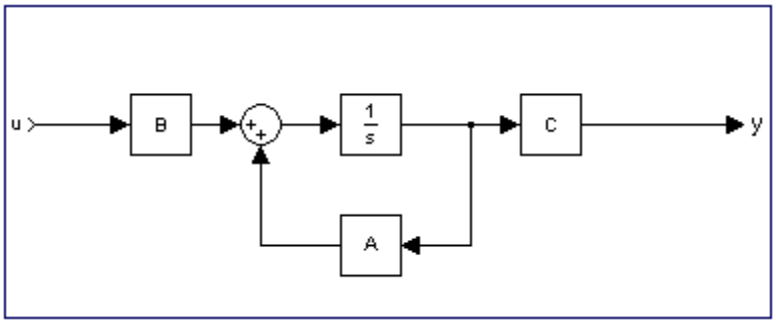

Figure 8 State Space Models – No Feed Forward (Toolbox, 2022)

The model parameters for the heat seal simulation are shown in Table 1. Inputs, outputs, and states are listed within the table.

Table 1 System Inputs, Outputs, and States

System Parameters	Designation	Matrix Vector	Function
Inputs (u)	*Th(t)*	*Bu(t)*	*Power input from the Heater*
	Tair (t)	*Bu(t)*	*Ambient Air temperature*
States (x)	*T1(t)*	*Ax(t)*	*Top of Medium Package Interface (MPI)*
	T2(t)	*Ax(t)*	*2nd Layer of MPI*
	T3(t)	*Ax(t)*	*3rd Layer of MPI*
	T4(t)	*Ax(t)*	*Top of Package*
Outputs (y)	*T1(t)*	*Cx(t)*	*Top of Medium Package Interface (MPI)*
	T2(t)	*Cx(t)*	*2nd Layer of MPI*
	T3(t)	*Cx(t)*	*3rd Layer of MPI*
	T4(t)	*Cx(t)*	*Top of Package*

The MATLAB program variables are listed in Table 2..

Table 2 MATLAB Variables Names

cal	Aluminum Specific Heat J/g C°
cpet	Polyethylene Terephthalate [PET] Specific Heat J/g C°
chsl	Heat seal lacquers Specific Heat J/g C°
cpvc	Polyvinylchloride Specific Heat J/g-C°
kh	Stainless Steel with thermal conductivity W/m C°
kal	Initial Aluminum thermal conductivity W/m C°
kpet	Polyethylene Terephthalate [PET] thermal conductivity W/m C°
khsl	Heat seal lacquers thermal conductivity W/m C°
kpvc	Polyvinylchloride thermal conductivity [PVC] W/m C°
lal	Length of Aluminum
lpet	length Polyethylene Terephthalate [PET]
lhsl	length Heat seal lacquers
lpvc	Initial length of Polyvinylchloride
lhmpi	Length from thermocouple to Medium Package Interface (MPI)
csah	Cross Sectional Area m^2
csca	Cross Sectional contact area sealing
mal	Mass Aluminum
mpet	Mass Polystyrene
mhsl	Mass Heat seal lacquers
mpvc	Mass Polyvinylchloride

The heat seal model will be constructed from the combination of the first-principal equations (1) and (2), the combination is labeled (4) through (7); these equations constitute the "A" matrix of the state space model.

$$\frac{dT_1}{dt} = -\frac{kal * csca * (T_1 - T_2)}{mal * cal * lal} + \frac{kh * csah * (T_h - T_1)}{mal * cal * lhmpi} \quad (4)$$

$$\frac{dT_2}{dt} = -\frac{kpet * csca * (T_2 - T_3)}{mpet * cpet * lpet} + \frac{kal * csca * (T_1 - T_2)}{mpet * cpet * lal} \quad (5)$$

$$\frac{dT_3}{dt} = -\frac{khsl * csca * (T_3 - T_4)}{mhsl * chsl * lhsl} + \frac{kpet * csca * (T_2 - T_3)}{mhsl * chsl * lpet} \quad (6)$$

$$\frac{dT_4}{dt} = -\frac{kpvc * csca * (T_4 - T_{air})}{mpvc * cpvc * lpvc} + \frac{khsl * csca * (T_3 - T_4)}{mpvc * cpvc * lhsl} \quad (7)$$

3.4 Heat Seal Model Assumptions

Certain assumptions were made for the simulation of this model and are specified below. The package is bounded within two surfaces and some of the variables related to these surfaces were assumed. There is some uncertainty pertaining to the contact area between the package and the barrier, so some assumptions were made.

3.4.1 Pressure

This model assumes that the pressure is sufficient to hold the materials together as shown in *Figure 9* (Clark, 2022).

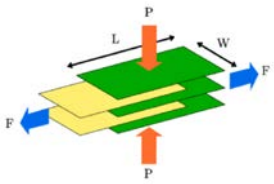

Figure 9 Pressure Multiple Levels (Clark, 2022)

3.4.2 Heater Block

When heat is applied to a polymer, it causes the chains within the polymer to vibrate. The heat seal energy must be sufficient to conduct through the entire thickness of each layer (Cooper, 2014).

The assumption is that the heater PID loop has been tuned so the setpoint is maintained at the desired temperature range at the time of contact. The PID loop provides the input power *Th(t)*; see Table 1, to the medium package interface (4). *Th(t)* comes from the heater system measurement instrument, which is a thermocouple, and it is displayed as the blue line in *Figure 12*.

By far the most common controller and analog process control used in industry is the Programmable Logic Controller [PLC]. This device has included a predesigned function block called “PID” and is used for proportional, integral, and derivative of a closed loop system. The PID loop shown below contains *Th(t)* in *Figure 10* (PID’S, 2015) (Mohammed).

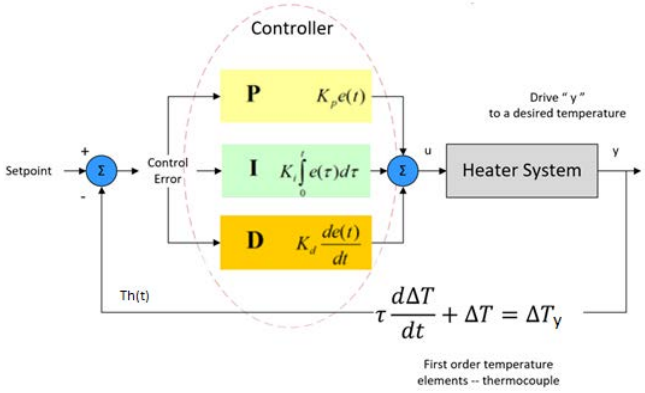

Figure 10 Heater PID Control (PID'S, 2015) (Mohammed)

3.4.3 Contact Area

The contact area between the heater die and foil will be assumed to have 100% heat transfer on the surface. As stated by Thermal Contact Resistance "Unfortunately, no universal model exists that can enable one to predict joint resistance between any two surfaces. To determine which of the available analytical models is appropriate for a situation, the thermal engineer must assess the surface conditions, addressing questions such as" Are the surfaces flat and/or rough? Are oxides on the surfaces? What is the pressure distribution within the contact? What is the real contact area? For surfaces where these questions can be answered with a high degree of certainty, some of the analytical models verified by extensive lab tests can be reliably used to predict overall thermal joint resistance" (Mantelli & Yovanovicht, 2022). This can be seen in *Figure 11* (Mantelli & Yovanovicht, 2022) where the heat is transferred only through the contact points, but due to irregularities the contact area is not 100%. There will be heat transfer by convection in the open area between layers, but this parameter will not be considered in this simulation.

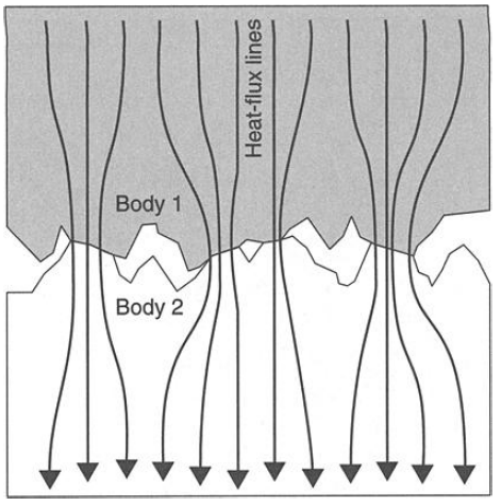

Figure 11 Heat Conduction through Contacting Points (Mantelli & Yovanovicht, 2022)

3.4.4 Material

Most "American Society for Testing and Materials" ASTM standards focus on testing the seal strength to determine the condition or quality of the seal (Mecmesin, 2022). Seal strength is equivalent to tensile strength and the units are measured in pascal (Pa) or newtons per square meter (N/m^2). There are many off-the shelf instruments or test assemblies that can be used to measure tensile strength. No suggestion of material properties or parameters that could be used for a design were mentioned in the ASTM standards. The combination of materials, when bonded, will determine seal strength. The simulation model temperature values are assumed to create the proper seal strength for the design.

3.5 Simulation Results Open Loop

Individual heat seal applications will have certain design criteria to meet system or process requirements. The data sets for this thesis simulation were comprised of synthetic data that simulate the design criterion that will concentrate on the *T4(t)* as the critical requirement; this is the temperature at the bottom of the medium package interface and the top of the package. This is shown within *Figure 5* Dairy Cup Sealing Layers Block Diagram and the results are shown in *Figure 12*.

Figure 12 shows a graph of one heat seal cycle. Concentrating on the legend on the bottom center shows *Th(t)*; this is the heater value produced by the PID loop discussed earlier. *T1(t)* through *T4(t)* are the various temperature levels; the Δ between each would be the temperature losses for a layer; this loss is determined by thermal resistances using Fourier's law of heat conduction (2). *Figure 12* also shows the rise and fall transient profile for each layer; this is determined by each individual layer's thermal capacitance using the first Law of Thermodynamics for a Close Loop System (3). *Figure 12* clearly shows that each layer's material properties influence each layer's losses, the transient profile, and thus the temperature profile associated with that layer.

The vertical lines in *Figure 12* depict contact time or dwell time, or the length of time that energy is applied to the material. Dwell time must be sufficient for heat to conduct through the material to the seal interface and long enough for the polymer to melt and for polymer chains to interact with one another (Darby, 2012) (Cooper, 2014).

After a set dwell time, the energy is removed from the heat-sealed films and the pressure is removed simultaneously. As stated in the assumption section, the temperature is sufficient to

hold the materials together. The heat seal remains hot after the removal of energy and pressure. Cooling time is another important factor because a heat seal is not fully strengthened until the polymer cools back down and crystals, if present, can re-form (Selke, Cutler, & Hernandez, 2004) (Cooper, 2014).

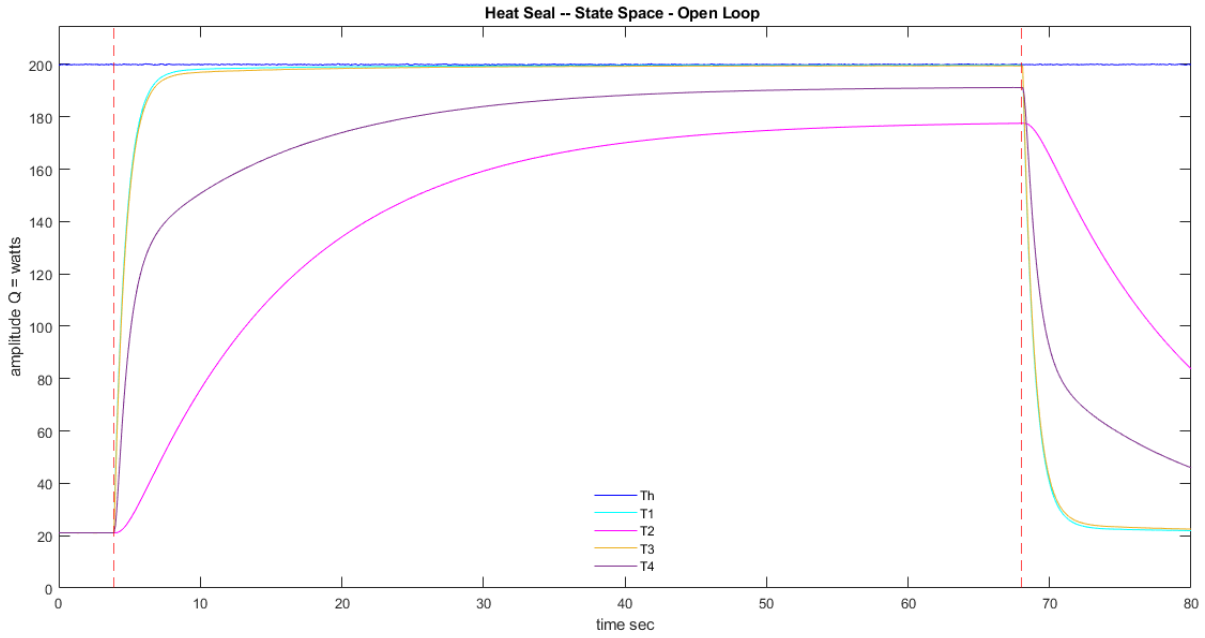

Figure 12 Heat Seal – State Space – Open Loop

CHAPTER 4: POLYNOMIAL / TRANSFER FUNCTION MODEL SIMPLIFICATION

The focus of this thesis is to input the data from the open-loop simulation into MATLAB's System Identification toolbox to determine the best-fit dynamical model, describing the relationships between the inputs and outputs of a system. Following the determination of the best-fit dynamical model, ANOVA statistical methods will be used to reduce the order or simplify the system. The lower ordered system will then be converted to a closed-loop state space system for analysis. There is ambiguity when changing from a physics-based model to a statistical model. There is uncertainty that the states of the original physics model will be maintained; but the assumption is, for this model, that the states are maintained.

4.1 Sample Size

To determine an appropriate sample size, the heat seal process will be examined for a 2-hour period of time. The machine has a cycle time of approximately 100 seconds that has an uptime efficiency of 80%, which equates to 57.6 cycles over a 2-hour period. Cochran's formula (Essa, 2021) will be used to determine sample size (5), assuming variability in the portion (p) is .5 and the z score for confidence level of 95% is 1.960.

$$n_o = \frac{Z^2 pq}{e^2} = \frac{1.9960^2 * .5 * .5}{0.05^2} \approx 385 \quad (5)$$

Because the assumed two-hour period permits at most N = 57.6 samples, which is less than Cochran's ideal sample size in (5), it becomes necessary to employ Cochran's small sample correction (Essa, 2021) (6)

$$n = \frac{n_o}{1 + \frac{n_o - 1}{N}} = \frac{385}{1 + \frac{384}{57.6}} \approx 50.2 \quad (6)$$

This work will simulate the first-principlas heat-seal system and synthesize 50 repetitions of input/output data as input to the system ID tool.

4.2 MATLAB System ID

Recall from Section 3.3 that the heat seal system is comprised of four coupled differential equations. The system inputs Th(t) and output T4(t) will be evaluated with the Autoregressive with Extra Input (*arx*) and Transfer Function (*tf*) models within the MATLAB System ID tool.

The *arx* tool will "estimate the parameters of a model using a least-squares method and the polynomial orders specified in [*23an b nk*]. Na is the order of polynomial A(q), specified as an Ny-by-Ny matrix, nb is the order of polynomial B(q) + 1, specified as an Ny-by-Nu matrix, nk is the input-output delay, also known as the transport delay, specified as an Ny-by-Nu matrix. (MathWorks, n.d.) (MathWorks, 2022). "The transfer function models describe the relationship between the inputs and outputs of a system using a ratio of polynomials. The model order is equal to the order of the denominator polynomial. The roots of the denominator polynomial are referred to as the model poles. The roots of the numerator polynomial are referred to as the model zeros" (MathWorks, 2022).

In an effort to determine if a lower-order model can be used, the one-way analysis of variance method (ANOVA) will be used to verify that 2nd through 8th order system models are equal. The stated null hypothesis is that all *arx* and Transfer Function models of 2nd , 4th , 6th and 8th order results of "best fit" will have equal means $H_0: \alpha_1 = \alpha_2 = \alpha_3 = \alpha_4$ against the alternative

hypothesis that at least one group is different from the others $H_1: \alpha_i \neq \alpha_j$. If the null hypothesis is confirmed the lowest order model can be used.

As determined by the sample size calculations, there were 50 program runs of a MATLAB-m file that created eight sets of synthetic data. Within each of the 50 program runs, the material parameters of thermal conductivity (W/m C°) were randomly varied per run by ± 5%. The percentage offsets are used to study the influence material properties have on the model. Included in the model are the inputs Th(t) and Tair(t) These inputs will be varied through the addition of white gaussian noise to each signal. The data sets are shown in boxes S1 through S8 within Figure 12.

The reasoning for the ± 5% offset is that when raw materials are purchased the properties of the materials are not exact, i.e., if you purchase a 64-onceliquid-filled container the volume is not exactly 64 ounces, there is some variation within the packing process.

As depicted by the arrows in *Figure 13* the first data set S1 was used to generate the *arx tf* models, *arx221* through *arx821* and *tf21* through *tf81*. The naming convention for *arx221* is [*24an b nk*] polynomial A(q), polynomial B(q) + 1, delay. The naming convention for *tf21* is [poles, zeros].

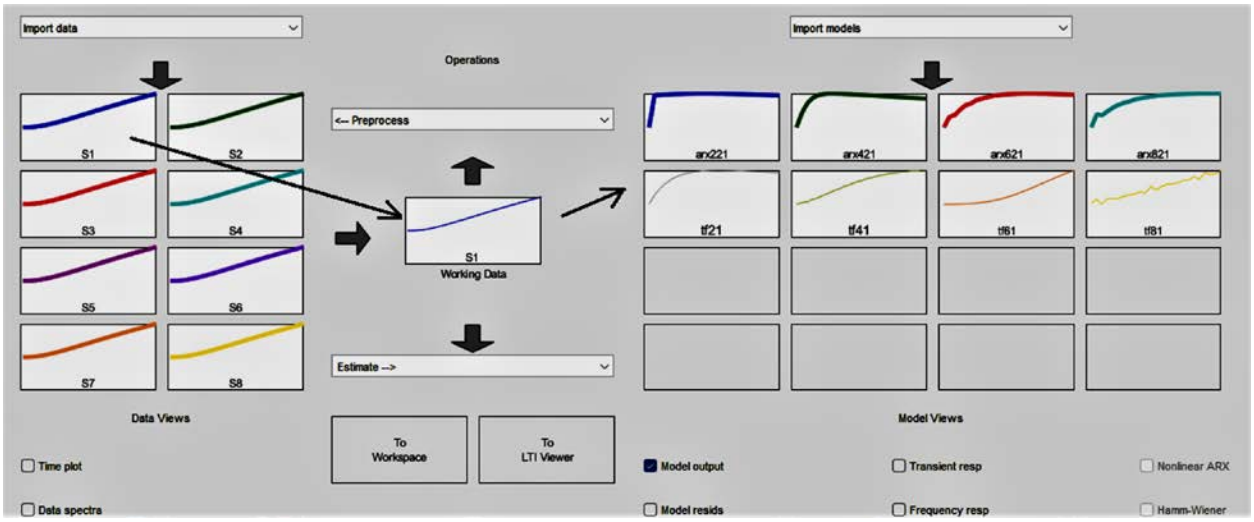

Figure 13 ± 5% Model Data Set

Figure 14 shows the best fit plots for S1, the first run of *arx* and *tf* models that are shown in *Figure 13*. All models have a greater than 98% best fit to what is considered the validation data set. By visual inspection, the transfer function *tf61* that contains six poles and one zero has the best fit.

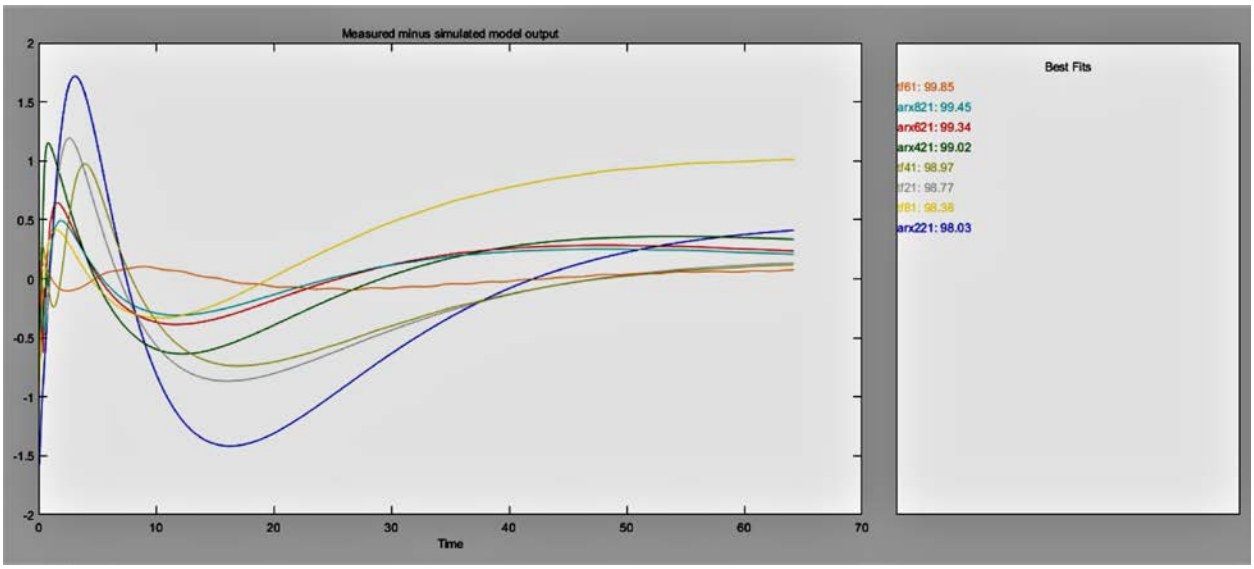

Figure 14 Best Fit Plots – S1 – *arx* and Transfer Function Models

4.3 ANOVA

The MATLAB m file was executed a total of 8 times with the eight sets of synthetic data; the data was ingested into the System ID tool to determine the "best fits" results for each data set are shown in Table 3 and in *Figure 15* through *Figure 21*. The results will be used to confirm the null hypothesis of the analysis of variance ANOVA test.

Table 3 System ID *arx* Best Fits

Runs	*arx*221	*arx*421	*arx*621	*arx*821	*tf*21	*tf*41	*tf*61	*tf*81
1	98.03	99.02	99.34	99.45	98.77	98.97	99.34	99.85
2	96.95	97.82	98.36	98.54	97.59	97.94	99.41	98.54
3	98.60	99.49	99.81	99.76	98.04	98.23	99.01	97.42
4	96.50	98.51	99.31	99.54	96.99	97.29	98.86	99.38
5	96.23	98.04	98.95	99.23	96.70	97.06	99.03	99.11
6	98.16	99.17	98.94	98.89	98.51	98.57	98.63	97.01
7	97.34	98.96	99.53	99.68	97.92	98.13	99.21	99.12
8	98.93	99.91	99.87	99.85	99.41	99.56	99.72	98.60

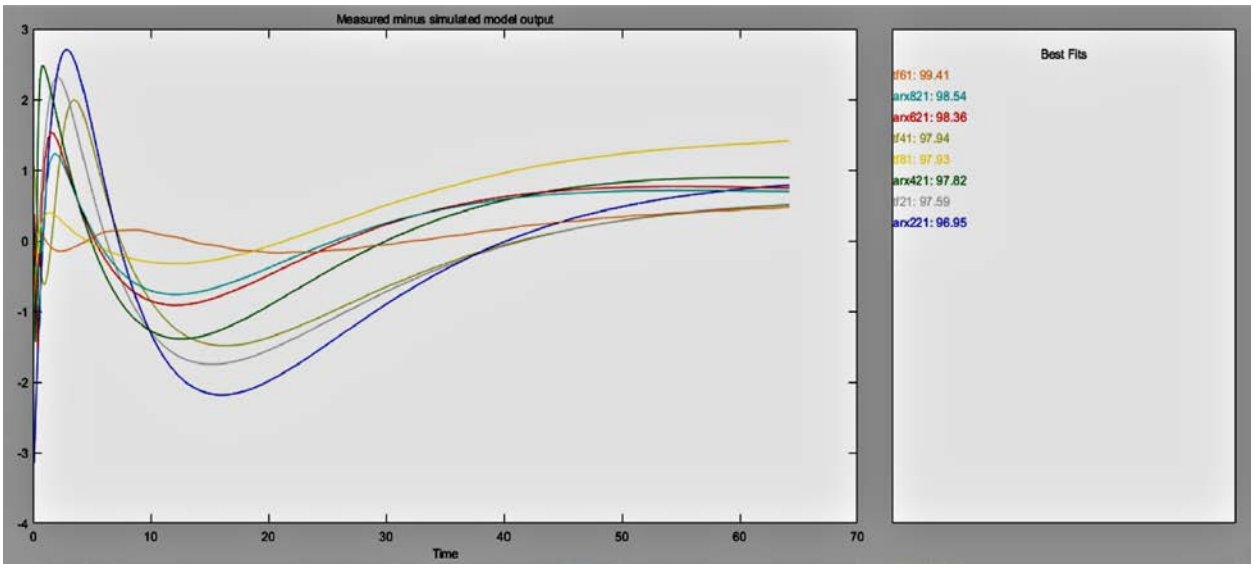

Figure 15 Best Fit Plots – S2 – *arx* and Transfer Function Models

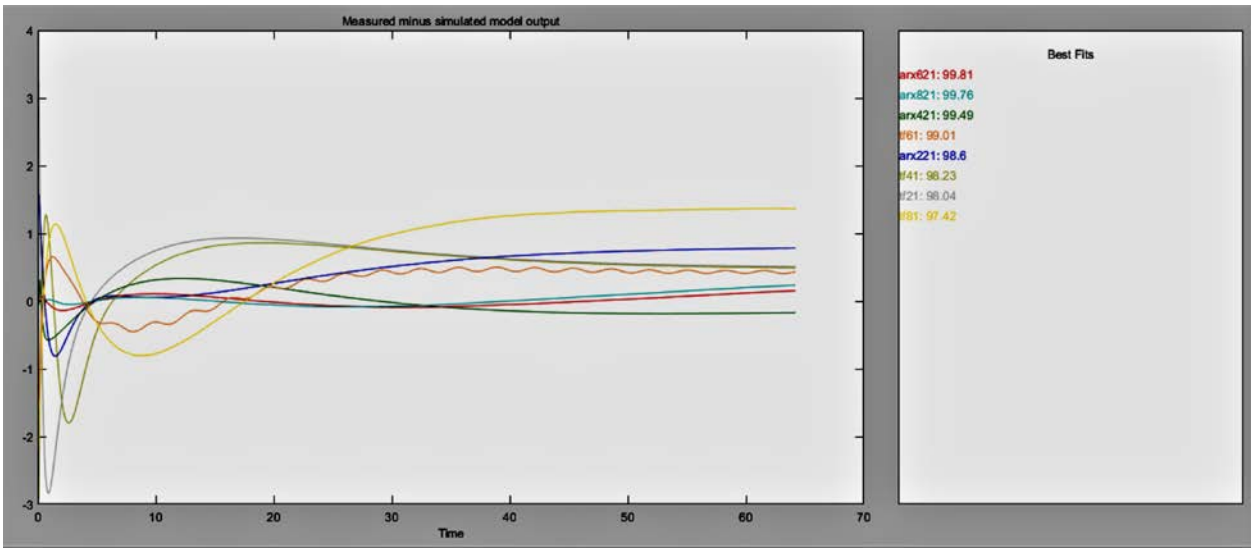

Figure 16 Best Fit Plots – S3 – *arx* and Transfer Function Models

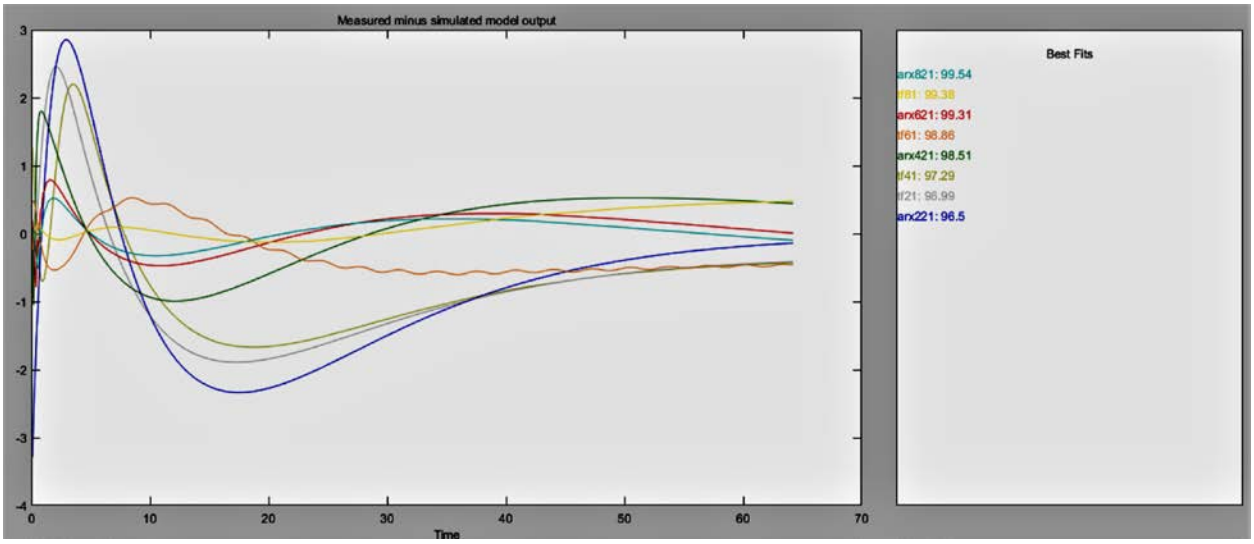

Figure 17 Best Fit Plots – S4 – *arx* and Transfer Function Models

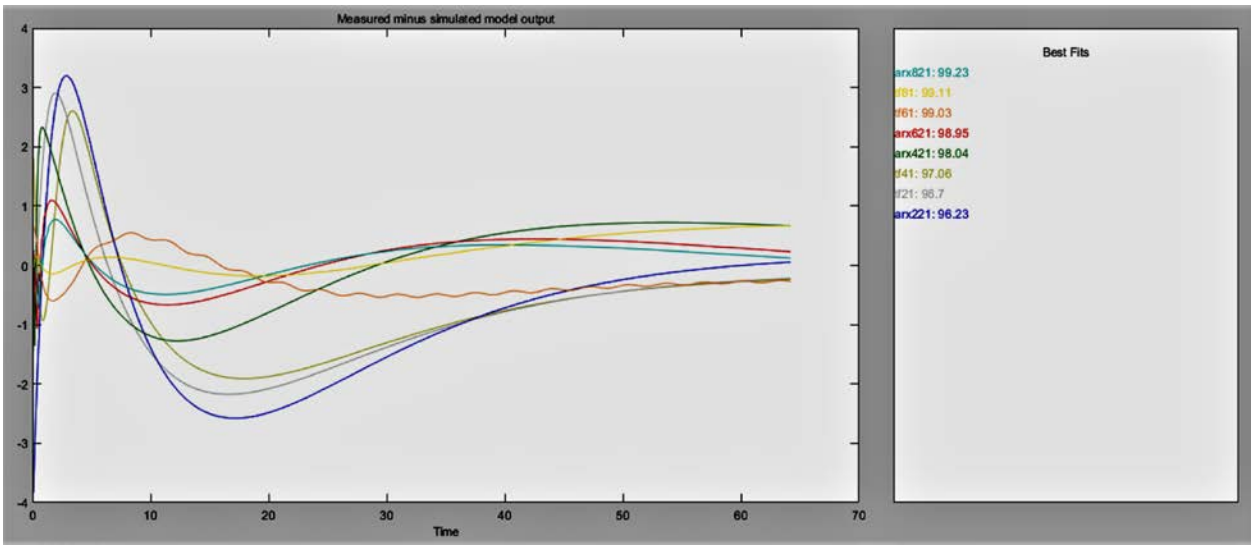

Figure 18 Best Fit Plots – S5 – *arx* and Transfer Function Models

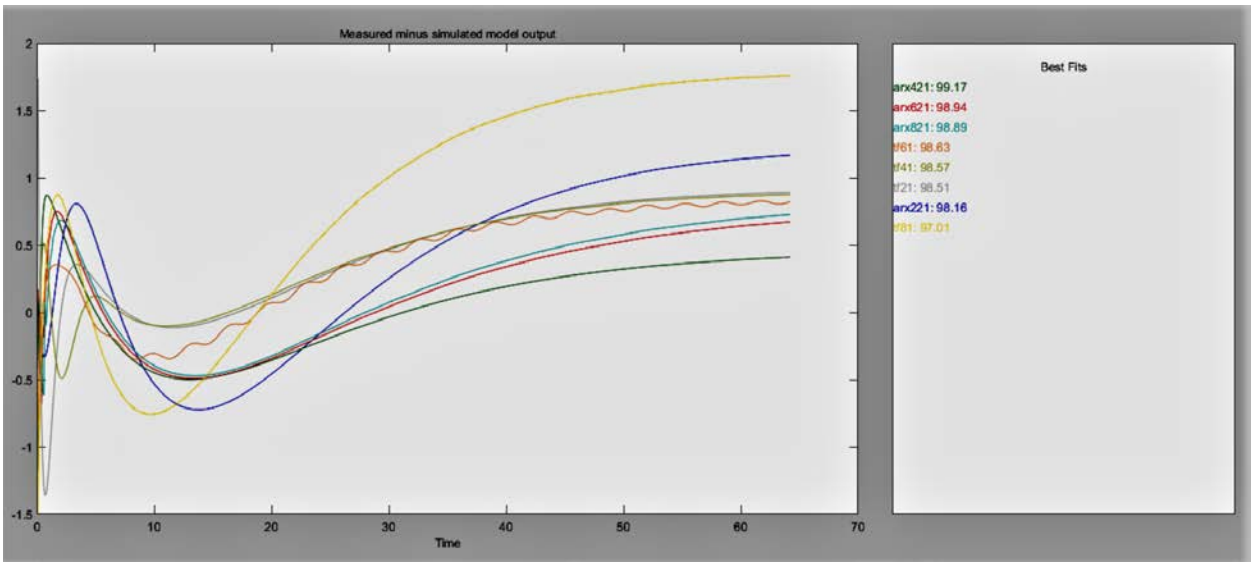

Figure 19 Best Fit Plots – S6 – *arx* and Transfer Function Models

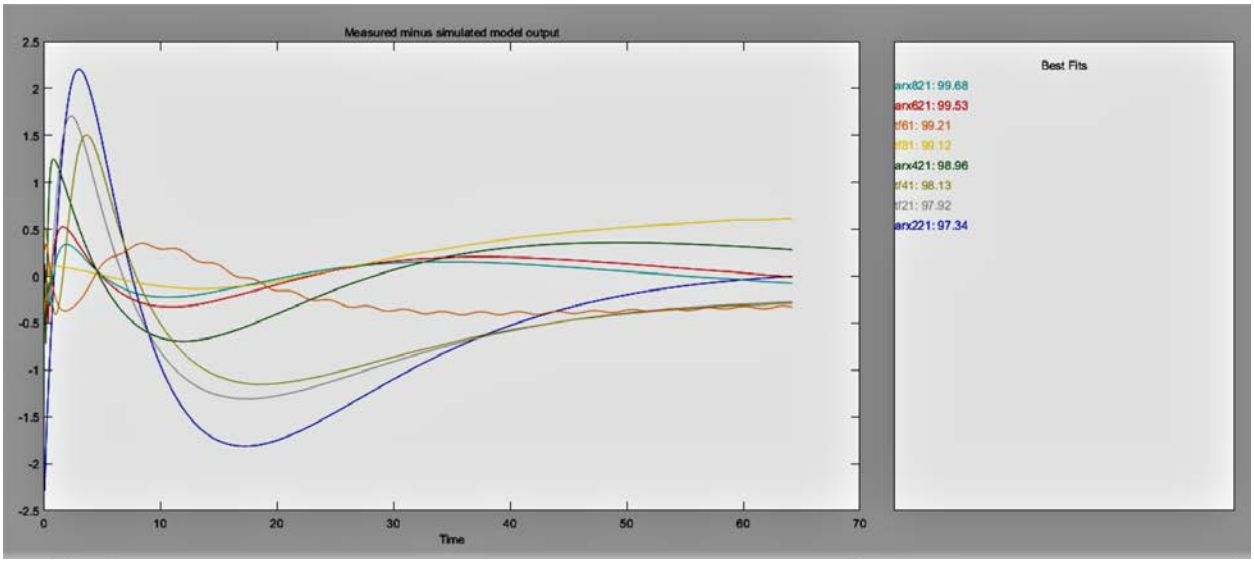

Figure 20 Best Fit Plots – S7 – *arx* and Transfer Function Models

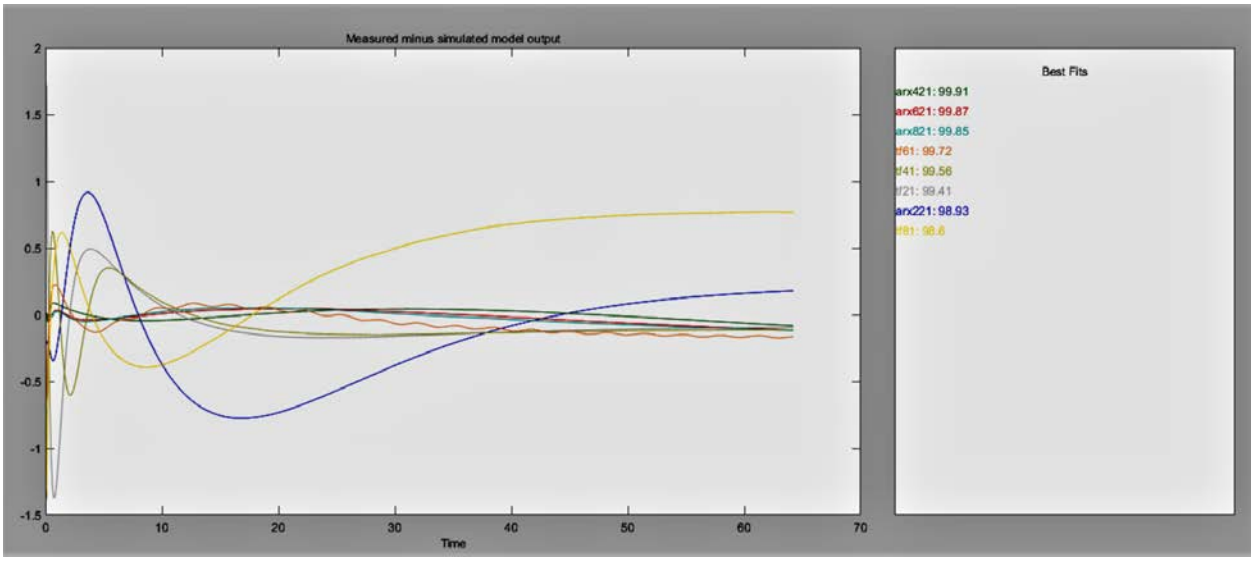

Figure 21 Best Fit Plots – S8 – *arx* and Transfer Function Models

Prior to examining the results for the analysis of variance (ANOVA) test, a determination is made if each order of the *arx* and Transfer function models results have a normal distribution. Using MATLAB " Anderson-Darling test, which returns a test decision for the null hypothesis that the data in vector x is from a population with a normal distribution. The alternative hypothesis is that x is not from a population with a normal distribution. If the logical result is 1, this test rejects the null hypothesis at the 5% significance level (MathWorks, 2022).

The results of the Anderson-Darling test for each of the eight data sets show a logical zero and P values greater than 0.05 for each. The results are shown in *Figure 22*, which accepts the Anderson-Darling null hypothesis that the data are within a normal distribution.

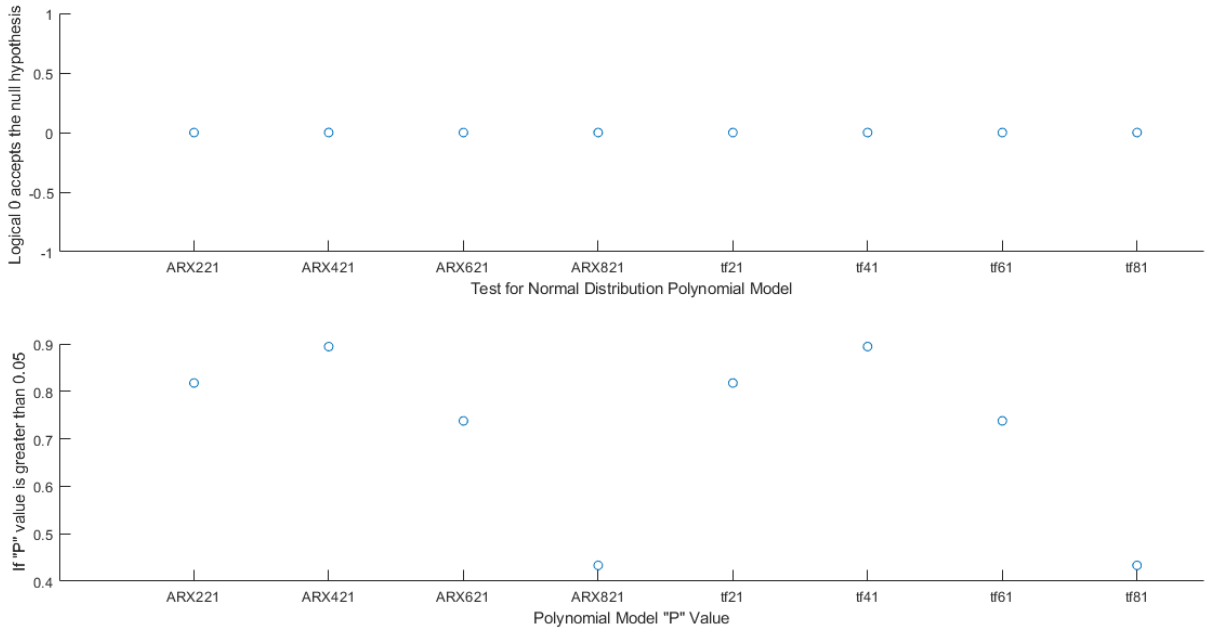

Figure 22 Anderson-Darling Test Logical and P Value Results

The analysis of variance (ANOVA) box plot shows from top to bottom within *Figure 23* the values Max, 75%-ile, median, 25%-ile and Min for each *arx* and transfer function order and the P-values of p1 = 0.8176, p2 = 0.8943, p3 = 0.7378, p4 = 0.4334, p5 = 0.9891, p6 = 0.9626, p7 = 0.9876, and p8 = 0.3816 which are all much greater than 0.05 so this confirms the null hypothesis that the data from this population has a normal distribution.

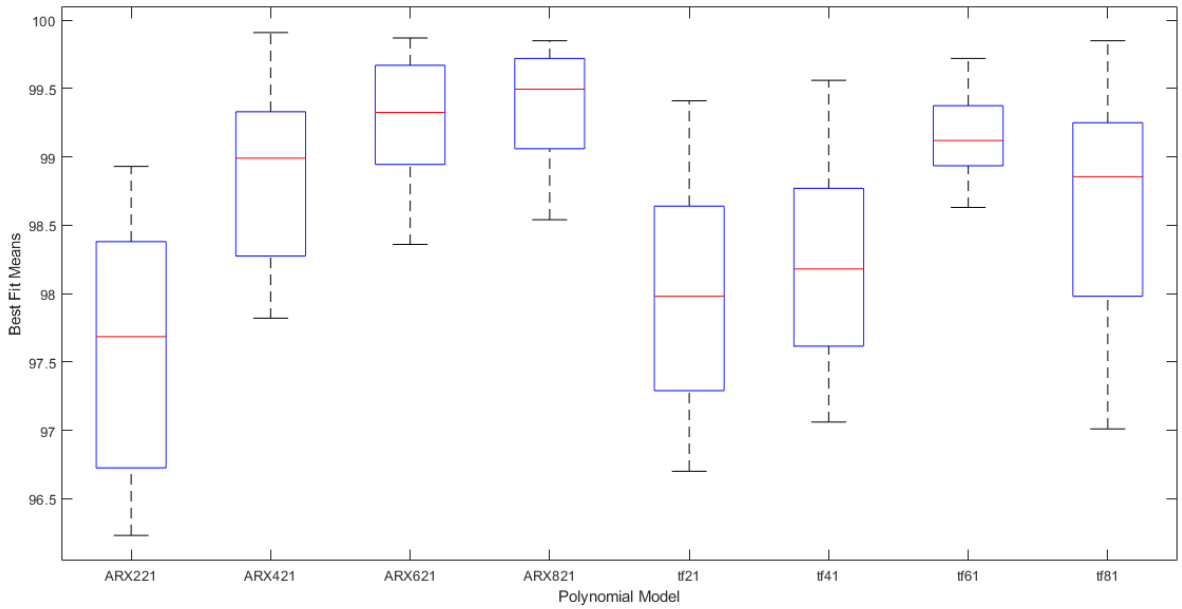

Figure 23 ANOVA Max, 75%-ile, median, 25%-ile and Min for Each Model.

Since the data was confirmed normal by the Anderson-Darling Test and the ANOVA null hypothesis was confirmed using the P-value all *arx* and transfer function models of 2^{nd} , 4^{th} , 6^{th} , and 8^{th} order results of "best fit" will have equal means $H_0: \alpha_1 = \alpha_2 = \alpha_3 = \alpha_4$ so the lowest or 2^{nd} order model can be used for close loop model simulation.

CHAPTER 5: STATE SPACE MODEL WITH FEEDBACK

There are numerous advantages control systems can bring to a manufacturing process: reduce scrap, increase yield, produce a better-quality product, and provide data for process analytics and machine reliability. Controller design is a well-studied discipline, providing systematic methods to firstly determine whether a targeted process is suitably constructed and instrumented to even support effective control. In the scope of this thesis, the key criteria are for the modeled process to be stable, controllable, and observable. The stability requirement is met by constraint within the system identification approach discussed in the preceding chapter, but how controllability and observability is verified is discussed in this chapter. Once the process is confirmed to meet these criteria, the next design decision is what algorithm to employ for controller synthesis: this chapter frames our heat-seal process failure recovery objective as an instance of the well-studied Linear-Quadratic Tracker (LQT)formulation under output feedback assumptions. Finally, this chapter concludes with a demonstration of the LQT solution approach in a simulated heat-seal failure scenario.

5.1 Controllability and Observability

To reliably meet control objectives, a system must be observed and controlled. Controllability is the property that, given any desired end state, there exists a control input by which the rendered state trajectory meets the end-state condition in a finite amount of time, no matter the initial state (Rutgers, 2022) . Controllability does not mean that the state must be maintained or held at that condition" (Douglas, State Space, Part 3: A Conceptual Approach to Controllability and Observability, 2022). The MATLAB tool "ctrb" was used to determine the controllability of a system using the matrixes A and B, the results concluded that the system is

controllable (MATLAB, Controllability matrix, 2022). Observability indicates that all critical states can be determined from the system outputs; see *Figure 24* (Douglas, State Space, Part 3: A Conceptual Approach to Controllability and Observability, 2022).

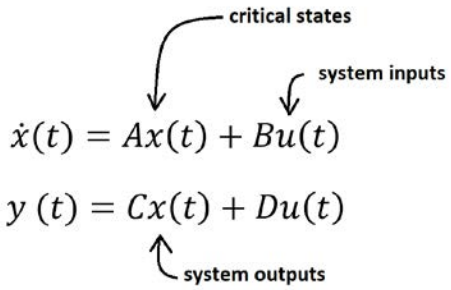

Figure 24 Critical States / System Outputs

In applications where measuring a critical state becomes impractical, then that state can be estimated by using a first principal equation or an observer. However, estimating states can be highly sensitive to modeling and measurement errors (Douglas, State Space, Part 3: A Conceptual Approach to Controllability and Observability, 2022) . For example, consider having only a position sensor but wanting access to the velocity, then the first-principle equation $\frac{d}{dt}position = velocity$ can be employed. However, if the position sensor does not have high accuracy, repeatability or the signal returned from the sensor contains noise, the velocity reading derived from this equation will also be in error and this could impact the controller's performance. One available tool to reduce the impact of noise is to employ a filter, most automation controls systems within industrial manufacturing use a programmable logic controller (PLC). The PLC has filters on analog input cards or averaging functions that can be programed to smooth out signal noise of the analog signal the system is capturing. MATLAB does have a tool to determine the observability "obsv", but this tool comes with a caution: "it is here for educational purposes and is not

recommended for serious control design" (MATLAB, Observability matrix, 2022), This MATLAB tool was used and determined this model is observable.

To illustrate at a high level the ideas of controllability and observability the system of a common bicycle will be studied, see *Figure 25* (Bikes, 2022) below.

Figure 25 Common Bicycle (Bikes, 2022)

Control devices for the bike are the handlebars, pedals, and brakes. Vision will be used for observation. When riding a bike without handlebars there will be no control mechanism to change the bike's direction, i.e., the bike is not controllable; but with vision the direction and speed can be observed, so the bike is observable. When riding the bike in complete darkness, the bike is controllable, but without vision there is no feedback on position, direction, or speed so the bike is not observable.

5.2 Model Stability

A state space model's stability is determined by the eigenvalues of its system matrix, A. Steve Brunton explains in detail the methods used to determine the stability of a system using

eigenvalues and eigen vectors (Brunton, Stability and Eigenvalues [Control Bootcamp], 2022) for both continuous and discrete time. If all eigenvalues in a continuous time system have negative-real part, then the system is stable; associated graphs of expected system responses are presented in *Figure 26* (Mossa, 2021, 13, 502–532).

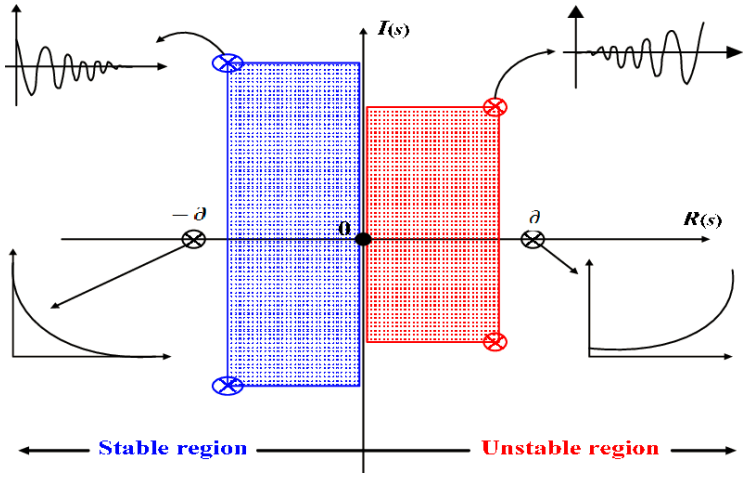

Figure 26 Linear Stability Analysis (Mossa, 2021, 13, 502–532)

An instrument is a device that measures or manipulates process physical variables. Instrumentation plays a significant role in both gathering information from the field and changing the field parameters, and as such are a key part of control loops. (Community, 2022). When reading data from instrumentation industrial process control systems update the data on a change of state or a fixed time period due to their design therefor the data in not continuous in nature, so this model's stability approach will be in a fixed Δ time or discrete time mode (Brunton, Linear Systems [Control Bootcamp], 2022). The radius of the eigenvalues will determine the system stability of a system; therefore, the magnitude of the eigenvalues must be inside the unit circle for stability; see *Figure 27* (Wang, 2022).

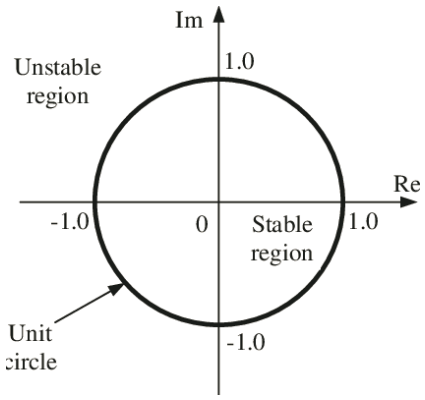

Figure 27 Stability Unit Circle (Wang, 2022)

Refereeing back to the 8 data sets created using the MATLAB system ID toolbox (MathWorks, 2022) and to the polynomial *arx* and transfer functions. An examination of the 2^{nd} , 4^{th}, 6^{th}, and 8th order responses of the discrete time system show all eigenvalues are inside the unit circle and the system would be considered stable, the results a shown in *Figure 28.*

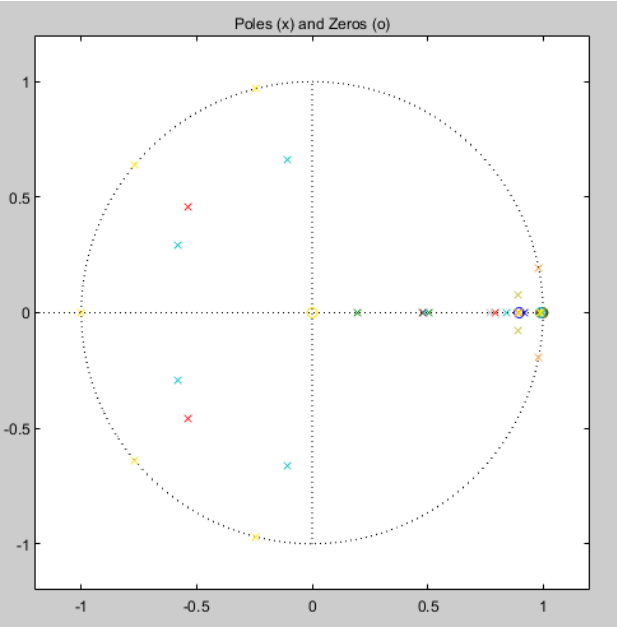

Figure 28 System ID Unit Circle Pole / Zero Plot

5.3 Linear Quadratic Regulator (LQR)

As discussed in the stability section, if a state-space model's A matrix shows eigenvalues that are unstable, then there are control methods like Pole Placement or Linear Quadratic Regulator (LQR) that can stabilize the system. *Figure 29* (Douglas, State Space, Part 4: What Is LQR Control, 2022) shows a schematic of both systems, as can be seen both diagrams are identical, but they differ in the approach to set the values of the controller's gain matrix K.

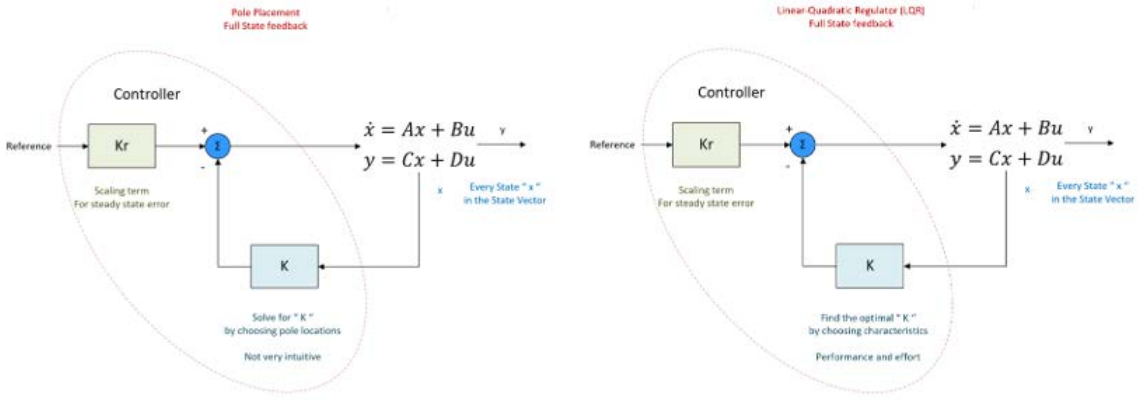

Figure 29 Pole Placement and LQR Control (Douglas, State Space, Part 4: What Is LQR Control, 2022)

5.4 Linear Quadratic Regulator (LQR) Stability

The State Space model displaying the placement of the K values in the feedback loop is shown in *Figure 30* (Toolbox, 2022).

Brian Douglas within a MATLAB tech talk (MATLAB, Eigenvalues and eigenvectors, 2022) breaks down pole placement at a high level. Pole placement works on the characteristic equation to modify the eigen values of the A matrix to change the dynamics of the system with the K matrix. This transformation will modify how energy is stored or moved within a system to guarantee stability; it can remove oscillations, speed up or slow down the dissipation of energy; this method in not used extensively in industry.

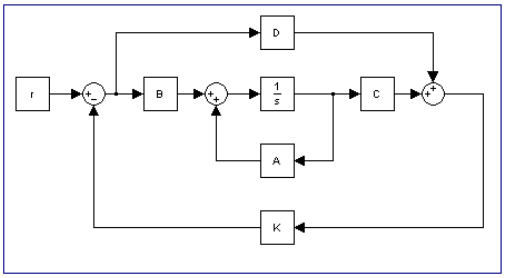

Figure 30 LQR State Space Model (Toolbox, 2022)

5.5 Linear Quadratic Regulator (LQR) Performance and Effort

Figure 29 shows the Pole placement and Linear Quadric Regulator designs have identical system diagrams but for Linear Quadric Regulator the K value is based on system performance and effort rather than choosing specific pole locations. Examining *Figure 31* (Douglas, State Space, Part 4: What Is LQR Control, 2022) shows an integral equation that contains the states [x] and the system inputs [u]. The values placed in the Q or R matrix will punish the performance and or effort of the system; this is done by increasing the values of Q and or R.

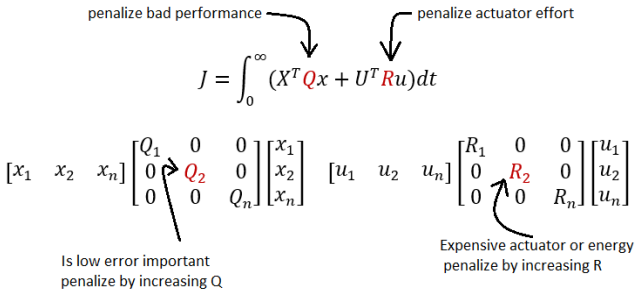

Figure 31 Performance [Q] and Effort [R] (Douglas, State Space, Part 4: What Is LQR Control, 2022)

Paralleling an example given by Brian Douglas (Douglas, State Space, Part 4: What Is LQR Control, 2022) an imagined experiment is shown in *Figure 32* (MOM, 2022) (Dishwashers, 2022)

(News, 2022) (PJ, 2022) (Pinterest, 2022) Dinner Party Performance [Q] and Effort [R] example. Consider the options when cleaning up after having a dinner party, there are three options to choose from, doing the work by hand, using an automated dishwasher, or using a cleaning service. Increasing the values of performance [Q] and Effort [R] will determine which option is chosen. Penalizing time, the option chosen is the cleaning service; Penalizing money, the option chosen is the dishwasher.

Dinner Party Cleanup

$$J = Q * time + R * dollars = J(cost)$$

Q = penalize time				
Q	Time	R	Dollars	cost
10	120 minutes	2	$3	1206
10	60 minutes	2	$10	620
10	5 minutes	2	$200	420
R = penalize dollars				
2	120 minutes	10	$3	270
2	60 minutes	10	$10	220
2	5 minutes	10	$200	2010

Figure 32 Dinner Party Performance [Q] and Effort [R] *Figure 32* (MOM, 2022) (Dishwashers, 2022) (News, 2022) (PJ, 2022) (Pinterest, 2022)

5.6 Linear Quadratic Tracker (LQT)

A natural extension of the Linear Quadratic Regulator (LQR) is the Linear Quadratic Tracker (LQT) (Bohner & Wintz, 2022). The aim of LQT algorithm will be to make the state vector x_i track as closely as possible a nominal state-vector $\hat{x_i}$, but subject to the control vector u_i

that tracks the nominal control vector $\widehat{u_t}$ (Pindyck, 1972). In our heat-seal context, the controller strives to follow an admissible control input trajectory Th that will generate a corresponding state trajectory T1, T2, T3 and T4. $\widehat{T4}$ such that the cost functional *J(u)* is minimized. As with LQR, the LQT matrices Q and R are the weights that are entered the quadratic cost function as shown in (8).

$$J = \int_0^T ((x - x_0)' Q(x - x_0) + (u - u_0)' R(u - u_0))dt \quad (8)$$

In the context of a heat seal, only the T4 state needs to be tracked. This results in the adoption of the LQT strategy under output feedback, not state feedback. LQT under output feedback is not well-solved by choice of a single gain matrix K, as is the case for LQR formulations under full-state feedback assumptions. The LQT tracking problem turns out to be well-posed only under discrete-time, finite horizon assumptions, which fortunately befits the experimental data we assumed for the heat-seal process. The solution is not just one gain matrix K for all time, but rather a trajectory of gain matrices that vary with the time samples. (O. Patrick Kreidl, 2022).

5.7 Simulation Experiments

This simulation will be using *T4(t)* as the critical temperature. Our experiments firstly assume that the shaded area that surrounds the 2nd order curve in *Figure 33* defines the regime of a good seal. This curve *T4(t)* was created using the pulsed input as shown by the input *Th(t)*, while the simulator was configured to represent truly the good sealing process.

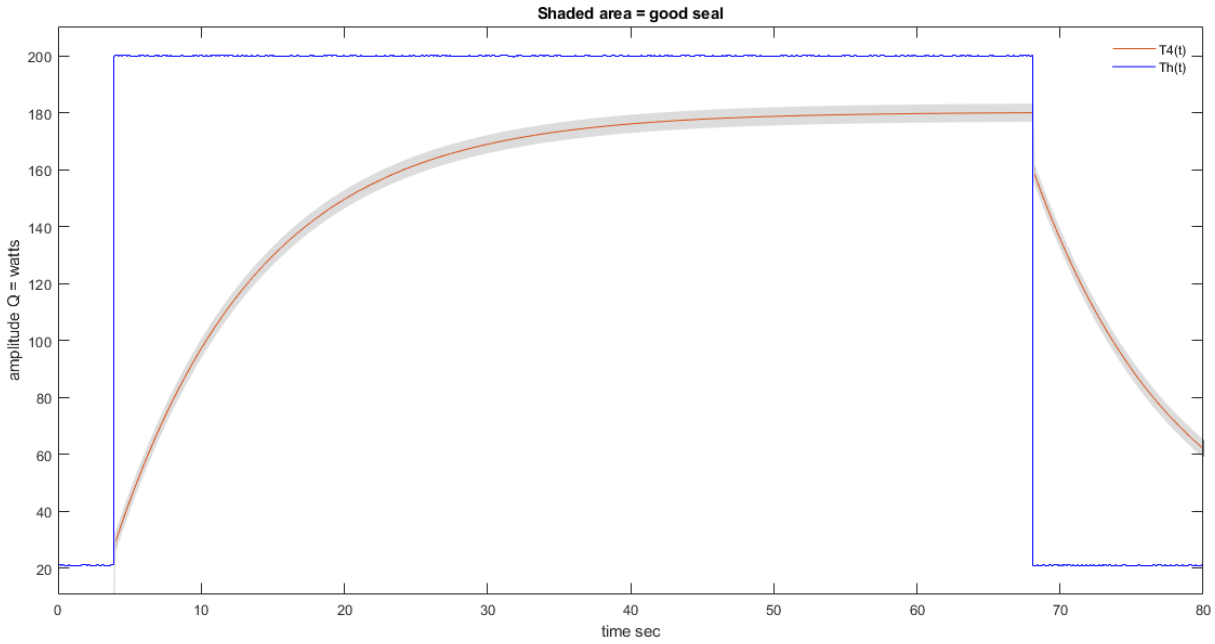

Figure 33 Good Profile

The simulator was reconfigured to render two curves that fall outside of the good-seal regime; specifically, these “bad-seal” curves were created by modifying material parameters for thermal conductivity. The first curve had its parameters modified to cause the function to drop below the deviation window, shown in *Figure 34*, while the second curve had parameter changes that placed this system above this window, shown in *Figure 35*.

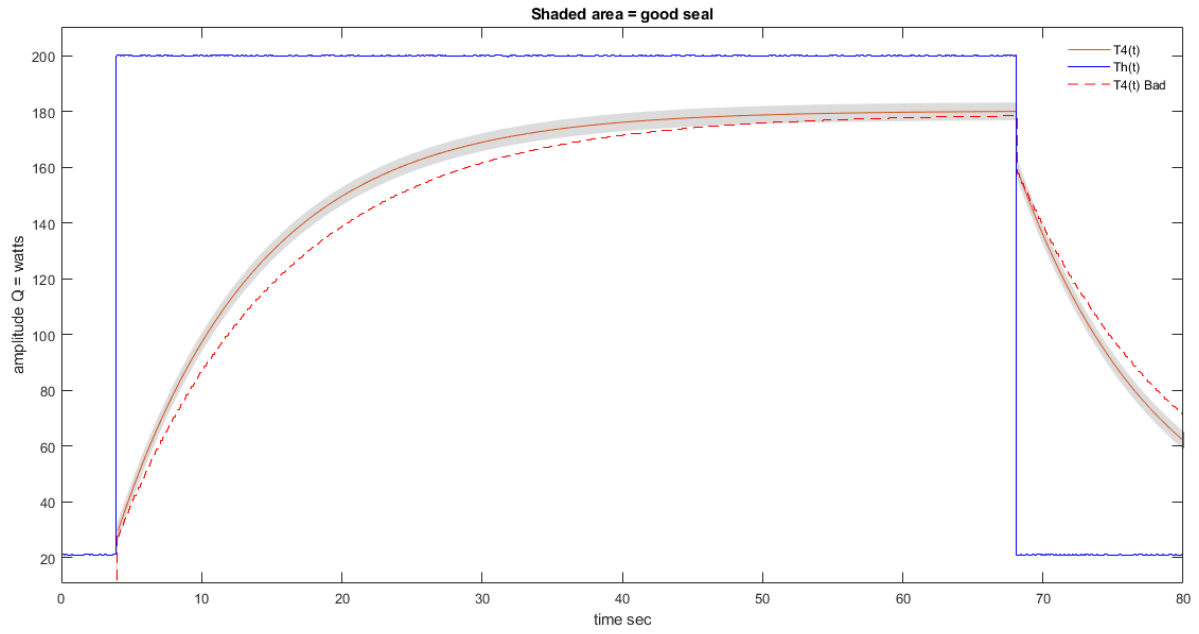

Figure 34 Bad Profile Below

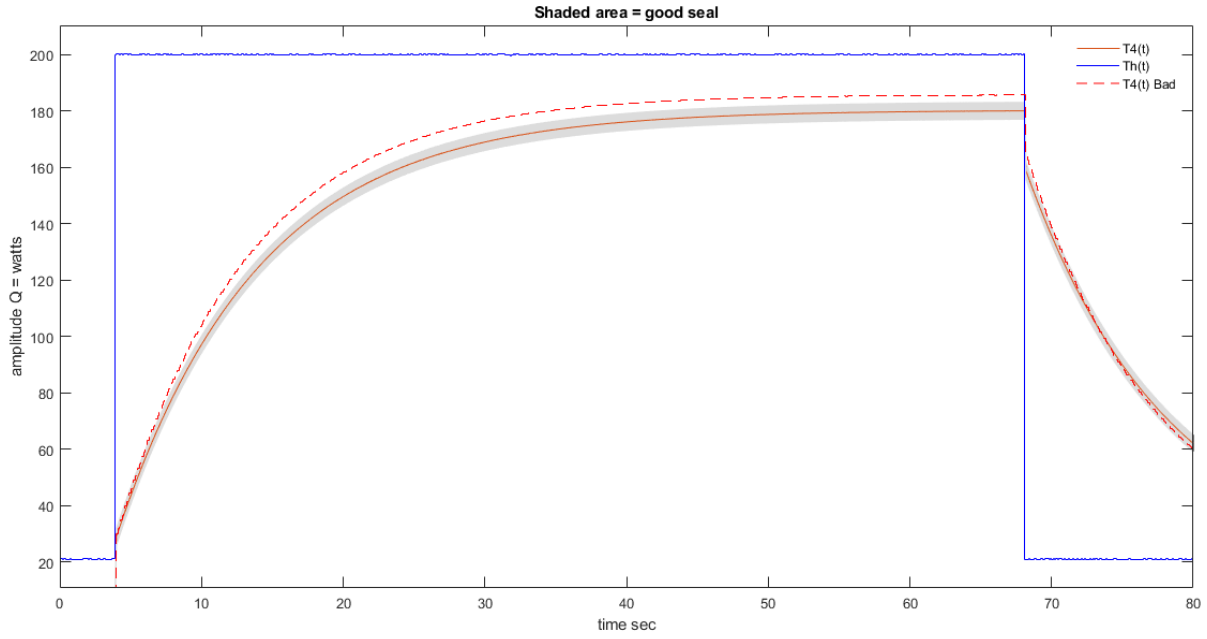

Figure 35 Bad Profile Above

Figure 37 and *Figure 38* shows three different LQT controller designs to recover from each simulated heat-seal failure. For each failure, the matrix R (that weighs the penalty of control effort)

was set equal to 1 and the matrix Q (that weighs the penalty of deviation from the good-seal) was varied.

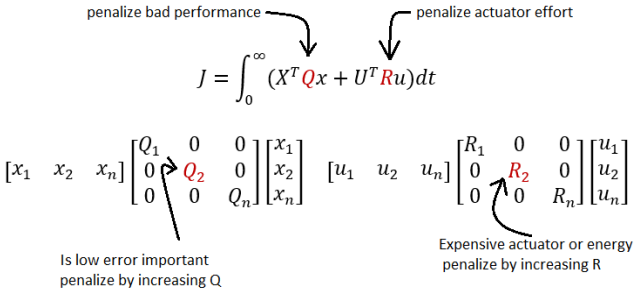

Figure 36 Performance [Q] and Effort [R]

The results show that as Q was increased, the Th(t) profile changed considerably to move the Th(t) "bad" to within the highlighted area that was considered good. The calculated penalties used the Euclidean norm, which is the distance of a vector from its original as shown in (9) (MATHWORKS, 2022).

$$\|v\| = \sqrt{\sum_{k=1}^{N} |v_k|^2} \quad (9)$$

In all cases, as weight Q increases relative to R, the error of Th increases while the error in T4 decreases; the highest value of Q =100 is shown on *Figure 37* and *Figure 38*, which shows T4 nearly identical to that of the good-seal response at the expense of noticeable deviation in Th from the simple pulse that was originally used.

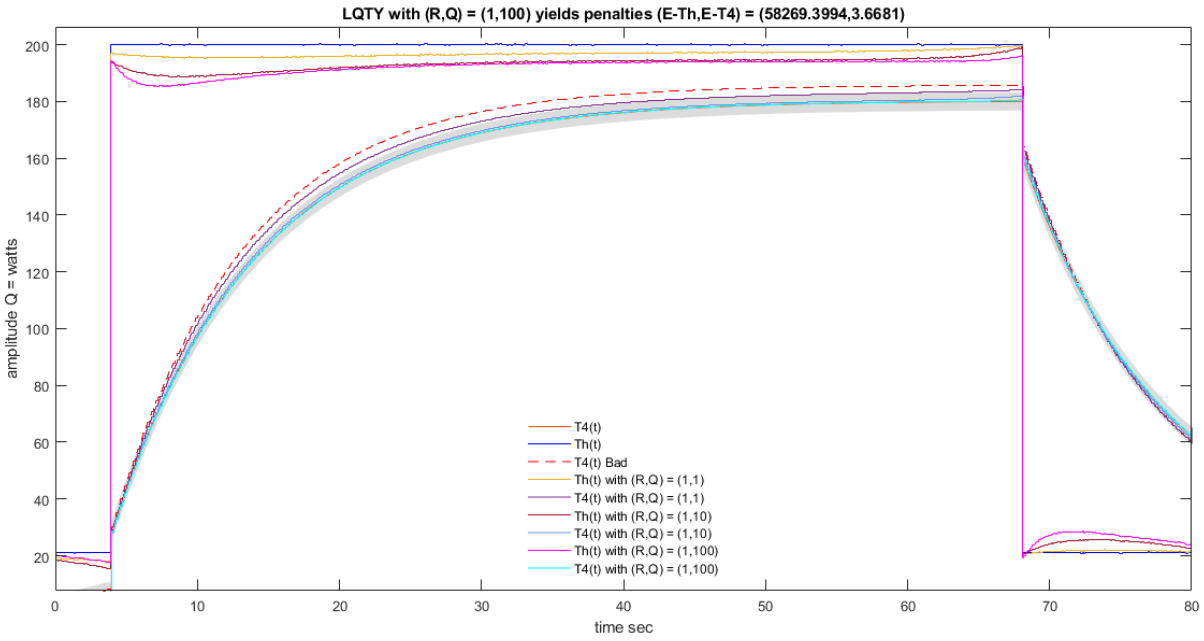

Figure 37 LQTY Corrected Profile Below

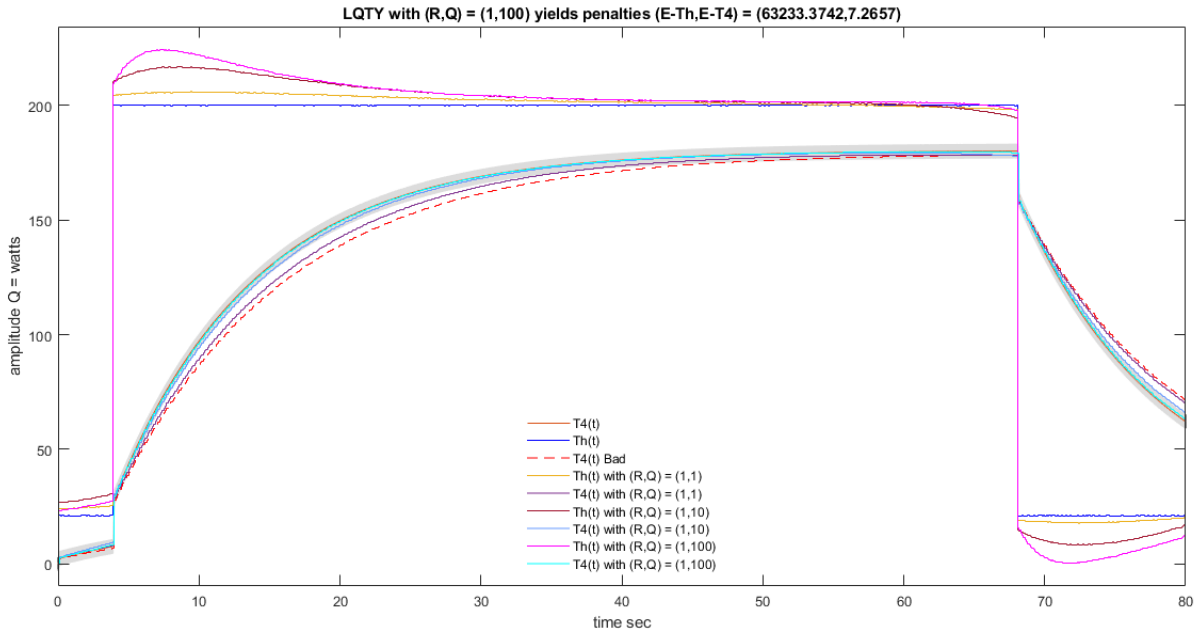

Figure 38 LQTY Corrected Profile Above

CHAPTER 6: CONCLUSION

The objective of this research was to present an idea for changing an existing long-standing process on how heat seal processes are verified. Performing a design of experiments may validate a system, but as a model-free approach it is near-impossible from DOE experiments alone to anticipate how material variations or other imposed system modifications may impact heat-seal quality.

The design of a state-space model comprised of first-principle equations that covered the layer-by-layer energy transfer of a fictitious package during the contact time when heat was applied. There was no existing test assembly or system that could be used for model setup, to emulate or to validate the simulation results against a real-world result, therefor assumptions that were made for the state space model. To gain insights and an understanding of the simulation program, parameters were varied by modifying the material variables; the realization became apparent that material modifications could change the systems performance considerably. Unless the simulation is verified the large system changes viewed in the simulation are an unknown, but the model was built using well-tried tools like state space modeling and first-principle equations. To show the capability of an open loop simulation, a 5% material variation was included in the model. Running this simulation exposed the temperature values at each layer; see *Figure 12*. Due to the constraints of current technology, only package or sensor destructive testing is available to measure the temperature on the last layer. The simulation could be applied to a known or new material and could reduce or eliminate the need for running a DOE. The simulation would have to be verified in a real-world process.

Examining the capability of a closed loop simulation using a fictitious sensor while using the Linear-Quadratic-Tracker controller design was demonstrated on two simulated “bad-seal” processes. It was shown to intuitively tradeoff the penalty of deviations from the good-seal response against the penalty of deviations from the original pulse heater input, refer to *Figure 34* and *Figure 35*. Settings for material parameters for the closed loop simulation were shifted for all four layers in thermal conductivity. These changes were on top of the 5% material variation included in the model. The odds are low this could be a possibility in real life; for instance, choosing the wrong material package interface or another alternative would be the modifications of the system, which was the motivation for this thesis. With the LQT function running continuously, a system would have the capability to correct and move a system back into compliance to create a good seal in real time, refer to *Figure 37* and *Figure 38*.

CHAPTER 7: FUTURE WORK

In order to continue to expand on this work, it is recommended that a researcher build a new or modify an existing heat seal test stand where the heat seal state-space open-loop model can be verified. One approach could be a modification to the heat seal dies or the package to allow an existing sensor to be placed in the sealing area so the temperature at the package to medium interface could be read; there would be a gap or void in the package, so this package could not be used in package integrity testing but the temperature on the last layer could be read to verify the model. Verification of this model could reduce the time needed to run a DOE protocol. If successful reading the last layer temperature, then there exist opportunities to develop an observer or an estimator that could estimate still-hidden states that may be relevant to diagnosing root-cause of heat-seal failures.

For the closed-loop model, there are a few areas that would have to be researched and tested. The first would be developing a temperature sensor that could withstand the pressure used within the sealing area and could maintain the seal integrity. A second area would be the design of a heater and die assembly where the profile developed by the LQT function could be realized. Another alternative would be to modify the LQT function that constrains the inputs to retain a pulse-shape, meaning the controller can change only the pulse-duration and pulse-height.

CHAPTER 8: BIBLIOGRAPHY

ADMET. (1994 - 2021). *Peel Strength Testing*. Retrieved from https://www.admet.com/peel-strength-testing/#:~:text=How%20To%20Measure%20Peel%20Strength,width%20of%20the%20bond%20line.

Adobe Stock. (2022). *Bridging the Gap*. Retrieved from https://stock.adobe.com/search?k=%22bridging+the+gap%22

Aithani, D., Lockhart, H., Auras, R., & Tanprasert, K. (2006). Heat Sealing Measurement by an Innovative Technique. *Packaging Technology and Science, vol. 19, no. 5*(Published online 5 May 2006 in Wiley InterScience (www.interscience.wiley.com).), pp. 245–257., doi:10.1002/pts.728.

American National Standards Institute. (2022, January). *ASTM F3039*. Retrieved from https://webstore.ansi.org/Standards/ASTM/astmf303915red

American Society For Quality. (2022). *What Is Design of Experiments (DOE)?* Retrieved from American Society For Quality: https://asq.org/quality-resources/design-of-experiments

Astrom, K. J. (2002). *Control System Design.* Retrieved from https://www.cds.caltech.edu: https://www.cds.caltech.edu/~murray/courses/cds101/fa02/caltech/astrom-ch4.pdf

Bahrami, M. (n.d.). *ENSC 388 (F09)*. Retrieved from Steady Conduction Heat Transfer: https://www.sfu.ca/~mbahrami/ENSC%20388/Notes/Staedy%20Conduction%20Heat%20Transfer.pdf

Bikes, L. (2022). *Somerset Smiles – Pulsium 3.0 Disc*. Retrieved March 2022, from https://www.lapierrebikes.com/gb-en/cycling-lifestyle/somerset-smiles-pulsium-3-0-disc/

Bohner, M., & Wintz, N. (2022, June). *Int. J. Dynamical Systems and Differential Equations, Vol. 3, No. 4, 2011*. Retrieved from Missouri University of Science and Technology: https://web.mst.edu/~bohner/papers/tlqtots.pdf

Brunton, S. (2022). *Linear Systems [Control Bootcamp].* Retrieved Feburary 1, 2022, from https://www.youtube.com/watch?v=nyqJJdhReiA&list=PLMrJAkhIeNNR20Mz-VpzgfQs5zrYi085m&index=2

Brunton, S. (2022). *Stability and Eigenvalues [Control Bootcamp].* Retrieved Feburary 1, 2022, from https://www.youtube.com/watch?v=h7nJ6ZL4Lf0&list=PLMrJAkhIeNNR20Mz-VpzgfQs5zrYi085m&index=6

Clark, A. (2022). *Pressure.* Retrieved from https://www.researchgate.net/figure/a-Layer-jamming-principle-With-a-pressure-applied-over-stacked-layers-force-F-is_fig2_347296413

Community, P. S.-E. (2022). *What is Instrumentation and Control ?* Retrieved from Inst Tools : https://instrumentationtools.com/what-is-instrumentation-and-control-engineering/

Cooper, R. (2014, December). *Microanalysis of Polymer Chain Diffusion in Heat Seals.* Retrieved March 2022, from https://tigerprints.clemson.edu/cgi/viewcontent.cgi?article=3042&context=all_theses

Corporate Finance Institute (n, d. (2022). *Statistics Fundamentals*. Retrieved from https://corporatefinanceinstitute.com/course/statistics-fundamentals/

Darby, D. (2012). Sealing technology for packaging processes. Unpublished manuscript.

Dishwashers, C. (2022). *Walmart.* Retrieved March 2022, from https://www.walmart.com/ip/Portable-Countertop-Dishwasher-5-Washing-

Programs/165471807?wmlspartner=wlpa&selectedSellerId=4192&&adid=22222222227362045791&wl0=&wl1=g&wl2=c&wl3=468512320463&wl4=pla-965769053436&wl5=9011566&wl6=&wl7=&wl8=&wl9=pla&wl10=1139400

Douglas, B. (2022). *State Space, Part 2: Pole Placement.* Retrieved December 2021, from https://www.youtube.com/watch?v=FXSpHy8LvmY

Douglas, B. (2022). *State Space, Part 3: A Conceptual Approach to Controllability and Observability.* Retrieved Feburary 1, 2022, from https://www.mathworks.com/videos/state-space-part-3-a-conceptual-approach-to-controllability-and-observability-1548327460100.html

Douglas, B. (2022). *State Space, Part 4: What Is LQR Control.* Retrieved December 2021, from https://www.youtube.com/watch?v=E_RDCFOlJx4

Engineering, B. E. (n.d.). *Feedforward Control.* Retrieved March 2022, from https://www.et.byu.edu/~tom/classes/436/ClassNotes/Class36(FeedforwardControl).pdf

Essa, P. (2021). *Cochran's formula for sample size* . Retrieved from youTube: https://www.youtube.com/watch?v=ggA-tEFM2bc

GeeksforGeeks. (2020). *One-Way ANOVA.* Retrieved from https://www.geeksforgeeks.org: https://www.geeksforgeeks.org/one-way-anova/

Grab, H. (2022). *Advanced Statistical Methods in Ecology*. Retrieved from https://heather-grab.github.io/Entom-4940/non-linear_w_poly.html

Gunter Schubert. (n.d.). *How Aluminium Foil Improves the Hot Tack of Packaging Laminates.* Retrieved from TAPPI: https://www.tappi.org/content/enewsletters/eplace/2007/06pla20.pdf

Heat Sealing Fundamentals, T. a. (2015). *WORCESTER POLYTECHNIC INSTITUTE*. Retrieved from https://web.wpi.edu/Pubs/E-project/Available/E-project-042915-173630/unrestricted/Heat_Sealing.pdf

Instron. (2022). *ASTM F88 Seal Strength of Flexible Barrier Materials*. Retrieved March 2022, from https://www.instron.com/en/testing-solutions/by-standard/astm/astm-f88---seal-strength

Instruments, W. T. (2022). *Differential Scanning Calorimeters*. Retrieved from https://www.tainstruments.com/products/thermal-analysis/differential-scanning-calorimeters/

Intellegens. (2022). *Design of experiments*. Retrieved March 2022, from https://intellegens.com/applications/software-data/design-of-experiments/

Lienhard, & Lienhard. (2019). *A Heat Transfer Textbook 5th Edition.* Cambridge Massachusetts: Phlogiston Press.

Mady, R., & Rutkowski, D. (2022). *Linear versus Non-linear models*. Retrieved from https://heather-grab.github.io/Entom-4940/non-linear_w_poly.html

Mantelli, M., & Yovanovicht, M. (2022). *Thermal Contact Resistance*. Retrieved Feburary 2022, from http://matthewwturner.com/uah/IPT2008_summer/baselines/LOW%20Files/Thermal/Spacecraft%20Thermal%20Control%20Handbook/16.pdf

MathWorks. (1994-2022). *State-space model*. Retrieved from State-space model: https://www.mathworks.com/help/control/ref/ss.html

MathWorks. (2022). *Anderson-Darling Test for a Normal Distribution*. Retrieved from https://www.mathworks.com/help/stats/adtest.html#btrbl9w-1

MathWorks. (2022). *Introduction to One-Way ANOVA.* Retrieved from https://www.mathworks.com/help/stats/one-way-anova.html

MATHWORKS. (2022, April). *lqry*. Retrieved from https://www.mathworks.com/help/control/ref/ss.lqry.html

MATHWORKS. (2022, June). *Norm*. Retrieved from Matlab: https://www.mathworks.com/help/matlab/ref/norm.html#bvhji30-1

MathWorks. (2022). *Polynomial Model Structure*. Retrieved from https://www.mathworks.com/help/ident/ug/what-are-polynomial-models.html

MathWorks. (2022). *System Identification Toolbox.* Retrieved December 2021, from https://www.mathworks.com/products/sysid.html

MathWorks. (2022). *Transfer Function Models*. Retrieved March 2022, from https://www.mathworks.com/help/ident/transfer-function-models.html?s_tid=CRUX_lftnav

MathWorks. (n.d.). *Estimate parameters of ARX, ARIX, AR, or ARI model*. Retrieved from https://www.mathworks.com/help/ident/ref/arx.html

MATLAB. (2022). *Controllability matrix.* Retrieved Feburary 1, 2022, from https://www.mathworks.com/help/control/ref/ss.ctrb.html

MATLAB. (2022). *Eigenvalues and eigenvectors.* Retrieved Feburary 2022, from https://www.mathworks.com/help/matlab/ref/eig.html

MATLAB. (2022). *Linear-Quadratic Regulator (LQR) design.* Retrieved December 2021, from https://www.mathworks.com/help/control/ref/lqr.html

MATLAB. (2022). *Observability matrix.* Retrieved Feburary 1, 2022, from https://www.mathworks.com/help/control/ref/ss.obsv.html

Mecmesin. (2022). *ASTM F88 standard test method for seal strength of flexible barrier materials*. Retrieved from Mecmesin: https://archive.mecmesin.com/astm-f88-standard-test-method-for-seal-strength-of-flexible-barrier-materials

Meka , P., & Stehling, F. (1994). Heat sealing of semicrystalline polymer films. Calculation and measurements of interfacial temperatures: effect of process variables on seal properties. *Journal of Applied Polymer Science*, 89–103 [DOI: 10.1002/app.1994.070510111].

Milivojevich, A. (2014). *How to calculate Statistical Process Control limits*. Retrieved from https://andrewmilivojevich.com/statistical-process-control-limits/

Mohammed, D. L. (n.d.). *Measurement & Control Instrumentations.* Retrieved from M.Sc. Production Engineering Course Department of Production Engineering & Metallurgy University of Technology: https://www.uotechnology.edu.iq/dep-production/laith/C&MI_lecture%202.pdf

MOM, T. O. (2022). *7 Tips for Creating Fewer Dirty Dishes*. Retrieved March 2022, from https://www.organizedmom.net/fewer-dirty-dishes/

Moresteam. (2022). *Design of Experiments (DOE)*. Retrieved from https://www.moresteam.com/toolbox/design-of-experiments.cfm

Moresteam. (2022). *Design of Experiments (DOE)*. Retrieved from https://www.moresteam.com/toolbox/design-of-experiments.cfm

Mossa, M. (2021, 13, 502–532). *Effective predictive current control for a sensorless five-phase induction motor drive. Int. J. Power Electron.* . Retrieved December 2021, from https://www.researchgate.net/figure/System-pole-positions-on-the-pole-zero-plot-see-online-version-for-colours_fig1_330635448

Mueller, c., Capaccio, G., Hiltner, A., & Baer, E. (1998). Heat Sealing of LLDPE: Relationships to Melting and Interdiffusion. *Department of Macromolecular Science and Center for Applied Polymer Research*,(B P Chemicals, Ltd., Applied Technology, Grangemouth, FK3 9XH, United Kingdom).

NAJARZADEH, Z. (2022). *CONTROL AND OPTIMIZATION OF SEALING LAYER IN FILMS*. Retrieved from http://docplayer.net/26050857-Control-and-optimization-of-sealing-layer-in-films.html

News, C. (2022). *Soap doesn't kill anything': How to hand wash your dishes and spread fewer germs.* Retrieved March https://www.ctvnews.ca/lifestyle/soap-doesn-t-kill-anything-how-to-hand-wash-your-dishes-and-spread-fewer-germs-1.4538098, 2022, from https://www.ctvnews.ca/lifestyle/soap-doesn-t-kill-anything-how-to-hand-wash-your-dishes-and-spread-fewer-germs-1.4538098

O. Patrick Kreidl, P. (2022, June). MATLAB code lqty. *Linear Quadratic Tracker*. Jacksonville, Florida, United States of America: Not published.

Packaging Foils. (2022). *Aluminium Foil based laminates for Packaging*. Retrieved from https://packagingfoils.com/alu-alu-foil-in-blister-packaging/

PID’S, T. A. (2015). *The Society of Aerial Cinematography*. Retrieved from https://thesoac.com/the-abcs-of-pids/

Pindyck, R. (1972). An Application of the Linear Quadratic Tracking Problem To Economic Stabilization Policy. *IEEE Transactions on Automatic Control*, Volume: 17, Issue: 3, pp. 387-400.

Pinterest. (2022). *Dishes Organization.* Retrieved March 2022, from https://id.pinterest.com/kenikmatan0908/dishes-organization/

PJ, M. C. (2022). *FaceBook.* Retrieved March 2022, from https://www.facebook.com/pjmaidcleaningservice/

Quality Assurance Solutions. (2022). *Attribute Sampling Plans*. Retrieved from https://www.quality-assurance-solutions.com/attribute-sampling.html

Rockwell Automation, Inc. (2022). *Serialization Makes Sense for Product Tracking and Traceability*. Retrieved from https://www.rockwellautomation.com/en-au/company/news/magazines/pharmaceutical-serialization-makes-sense-for-product-tracking-an.html

Rutgers. (2022). *Controllability and Observability.* Retrieved from https://www.ece.rutgers.edu/~gajic/psfiles/chap5traCO.pdf

Sami, M. (2022). *Personal website – Software Engineering & Architecture Practices*. Retrieved from https://melsatar.blog/2019/07/12/types-of-technological-changes/

Sand, C. K. (2022). *Testing the Integrity of Package Seals.* Retrieved from https://www.packagingtechnologyandresearch.com/uploads/2/4/1/1/24118835/0719_col_packaging.pdf

Science Direct. (2022). *Imaginary Axis - an overview | ScienceDirect Topics.* Retrieved March 2022, from https://www.sciencedirect.com/topics/computer-science/imaginary-axis/pdf

Sealer, I. I. (2022). *Heat Sealing for Medical and Pharmaceutical Products*. Retrieved from http://www.imsmachines.net/medical-heat-sealing/#.YjpMSOfMKPp

Selke, S., Cutler, J., & Hernandez, R. (2004). *Plastics packaging: Properties, processing, applications, and regulations (2nd ed.).* Cincinnati, Ohio: Hanser Publications.

ShareTechNote. (n.d.). *DE - State Space Modeling* . Retrieved from http://www.sharetechnote.com/html/DE_StateSpaceModel.html

Short, M., Pont, M., & Huang, Q. (2004/10/11). *Simulation of Vehicle Longitudinal Dynamics.*

Theller. (1989). Heat sealability of flexible web materials in hot-bar sealing applications. In Theller, *Plastic Film Sheeting* (pp. 66–93.).

Toolbox, L. (2022). *Statespace models*. Retrieved from https://www.lisamission.org/ltpda/usermanual/ug/ssm.html

Tsujii Tetsuya, e. a., Ishiaku, U. S., Mizoguchi, M., & Hamada, H. (2004). The Effect of Heat Sealing Temperature on the Properties of OPP/CPP Heat Seal. I. Mechanical Properties. *Journal of Applied Polymer Science, DOI 10.1002/app.21320*(Published online in Wiley InterScience (www.interscience.wiley.com).), 97. 753 - 760. 10.1002/app.21320. Retrieved from Wiley: www.interscience.wiley.com

Wang, J. (2022). *Stable and unstable regions for pole locations in the z plane.* Retrieved March 2022, from https://www.researchgate.net/figure/Stable-and-unstable-regions-for-pole-locations-in-the-z-plane_fig2_271920007

Webb, K. (2022). *SECTION 4: FIRST- AND SECOND-ORDER SYSTEMS.* Retrieved from https://web.engr.oregonstate.edu:

https://web.engr.oregonstate.edu/~webbky/ESE499_files/Section%204%20First-%20and%20Second-Order%20Systems.pdf

Wiley. (2021). *Understanding the factors affecting the seal integrity in heat sealed flexible food packages: A review*. Retrieved from Packaging Technology and Science an International Journal: https://onlinelibrary.wiley.com/doi/10.1002/pts.2564

CHAPTER 9: APPENDIX

9.1 MATLAB Code

```
% Author Charles Albanese
% University of North Florida MSEE Thesis
% 1 May 2022
clear; close all; clc;
% select number of samples
numSamples = 50; percentOffset = 0.05; stepSize = 0.1;
maxTime = 80; time = 0:stepSize:maxTime; lowPercent = 0.05;
highPercent = 0.85; Qin = 200; n1 = 1; n2 = 1;
%-------------Density (g/m^3)------------
dss     = 8000000;  % Stainless steel Density (g/m^3)
dal     = 2710000;  % density Aluminum is about g/m3.
dpet    = 1370000;  % density Polyethylene Terephthalate [PET] g/m3
dhsl    = 805000;   % Heat seal lacquers density g/m3
dpvc    = 1300000;  % density Polyvinylchloride g/m3
%--------------------------------
Tair    = (70-32)*(5/9);    %air temperature C°
QQin    = 1;
%-------------Specific Heat J/g C°-------------------------
ch      = 0.468;    % Specific Heat Capacity Steel  J/g-C°
cal     = 0.897;   % Aluminum Specific Heat J/g C°
cpet    = 1.350;   % Polyethylene Terephthalate [PET] Specific Heat J/g C°
chsl    = 1.000;   % Heat seal lacquers Specific Heat 1.011 to 1.369 J/g C°
cpvc    = 1.170;   % Polyvinylchloride Specific Heat J/g-C°
%--------------thermal conductivity  W/m C°--------------------
```

```
kh      = 16.3;    % stainless steel with thermal conductivity  W/m C° = j(s
m C°)
kal     = 238.0;   % Initial Aluminum Thermal conductivity (W/mC°) = j/(s m
C°)
kpet    = 0.23;    % Polyethylene Terephthalate [PET] Thermal conductivity
(W/mC°)
khsl    = 0.15;    % Heat seal lacquers Thermal conductivity  W/m C°
kpvc    = 0.11314; % Polyvinylchloride thermal conductivity W/m C°
%-----------distance-----------------------------
lhmpi   = 0.002032; % Length from thermocouple to Medium Package Interface
lh      = 0.254;    % Lenght of die
wh      = 0.254;    % Width sealing die
hgth    = 0.254;    % Height of sealing die =
lal     = 0.00762;  % Length of Aluminum
lsa     = 0.2032;   % length of sealing area
wsa     = 0.2032;   % width of sealing area
lpet    = 0.000254; % length Polyethylene Terephthalate [PET]
lhsl    = 0.000254; % length Heat seal lacquers
lpvc    = 0.00254;  % Initial length (lpvc) of Polyvinylchloride
% Create 10 seperate data models by varing material paramters.
% Create the 8 data sets for system ID Best Fit Models
% 2 data sets for LQTY analysis
while n1 <= 10
% n2 number of samples wihtin a data set
for n2 = 1:numSamples
% LQTY Anaylsis
if n1 == 9
```

```
%-------------------------------------------------------------
kal     = 230.0;   % Initial Aluminum Thermal conductivity (W/mC°) = j/(s m
C°)
kpet    = 0.20;    % Polyethylene Terephthalate [PET] Thermal conductivity
(W/mC°)
khsl    = 0.12;    % Heat seal lacquers Thermal conductivity  W/m C°
kpvc    = 0.10;    % Polyvinylchloride thermal conductivity W/m C°
%-------------------------------------------------------------
end
% LQTY Anaylsis
if n1 == 10
%-------------------------------------------------------------
kal     = 245.0;   % Initial Aluminum Thermal conductivity (W/mC°) = j/(s m
C°)
kpet    = 0.26;    % Polyethylene Terephthalate [PET] Thermal conductivity
(W/mC°)
khsl    = 0.17;    % Heat seal lacquers Thermal conductivity  W/m C°
kpvc    = 0.09;    % Polyvinylchloride thermal conductivity W/m C°
%-------------------------------------------------------------
end
% Randomly vary parameters
% Aluminum Specific Heat J/g C°
calMin     = (cal - (cal*percentOffset)); %Minimum
calMax     = (cal + (cal*percentOffset)); %Maximum
cal1        = calMin + ((calMax - calMin)* rand);
% Polyethylene Terephthalate [PET] Specific Heat J/g C°
cpetMin    = (cpet - (cpet*percentOffset)); %Minimum
```

```
cpetMax    = (cpet + (cpet*percentOffset)); %Maximum
cpet1       = cpetMin + ((cpetMax - cpetMin)* rand);
% Heat seal lacquers Specific Heat J/g C°
chslMin    = (chsl - (chsl*percentOffset)); %Minimum
chslMax    = (chsl + (chsl*percentOffset)); %Maximum
chsl1       = chslMin + ((chslMax - chslMin)* rand);
% Polyvinylchloride Specific Heat J/g-C°
cpvcMin    = (cpvc - (cpvc*percentOffset)); %Minimum
cpvcMax    = (cpvc + (cpvc*percentOffset)); %Maximum
cpvc1       = cpvcMin + ((cpvcMax - cpvcMin)* rand);
% Initial Aluminum Thermal conductivity (W/mC°) = j/(s m C°)
kalMin     = (kal - (kal*percentOffset)); %Minimum
kalMax     = (kal + (kal*percentOffset)); %Maximum
kal1        = kalMin + ((kalMax - kalMin)* rand);
% Polyethylene Terephthalate [PET] Thermal conductivity (W/mC°)
kpetMin    = (kpet - (kpet*percentOffset)); %Minimum
kpetMax    = (kpet + (kpet*percentOffset)); %Maximum
kpet1       = kpetMin + ((kpetMax - kpetMin)* rand);
% Heat seal lacquers Thermal conductivity  0.15 W/m C°
khslMin    = (khsl - (khsl*percentOffset)); %Minimum
khslMax    = (khsl + (khsl*percentOffset)); %Maximum
khsl1       = khslMin + ((khslMax - khslMin)* rand);
% Polyvinylchloride thermal conductivity W/m C°  PVC
kpvcMin    = (kpvc - (kpvc*percentOffset)); %Minimum inches
kpvcMax    = (kpvc + (kpvc*percentOffset)); %Maximum inches
kpvc1       = kpvcMin + ((kpvcMax - kpvcMin)* rand);
sah = (lh*wh*2)+(lh*hgth*2)+(2*wh*hgth);  % surface area of heater.
```

```
csah    = (wh*lh);  % Cross Sectional Area m2
csca    = (wh*lh)-(lsa*wsa);    % Cross Sectional contact area sealing
%--------------------
mh      = (dss*(csah*hgth));      % M = DV
mal     = (dal)*(csca*lal);     % Mass  = Density * Volume -- Aluminum
mpet    = (dpet )*(csca*lpet);   % Density  = Mass* Volume – Polystyrene
mhsl    = (dhsl)*(csca*lhsl );   % Mass  = Density * Volume  -- Heat seal
lacquers
mpvc    = (dpvc)*(csca*lpvc);       % Mass  = Density * Volume
%---------------------------------------------
%State Space
% dT1dt   = -(((kal*csca)/(mal*cal*lal))*(T1 - T2)) +
((kh*csah)/(mpet*cal*lhmpi))*(Th - T1)
AR1C1 = -(((kh*csah)/(mal*cal1*lhmpi))+((kal1*csca)/(mal*cal1*lal)));
%T1
AR1C2 = ((kal1*csca)/(mal*cal1*lal));
%T2
AR1C3 = 0;
%T3
AR1C4 = 0;
%T4
BR1C1 = ((kh*csah)/(mal*cal1*lhmpi));
%Qin
BR1C2 = 0;
%Tair
% dT2dt   = -(((kpet*csca)/(mpet*cpet*lpet))*(T2 - T3)) +
(((kal*csca)/(mpet*cpet*lal))*(T1 - T2))
```

```
AR2C1 = ((kal1*csca)/(mpet*cpet1*lal));
%T1
AR2C2 = -(((kal1*csca)/(mpet*cpet1*lal))+((kpet1
*csca)/(mpet*cpet1*lpet)));%T2
AR2C3 = ((kpet1 *csca)/(mpet*cpet1*lpet));
%T3
AR2C4 = 0;
%T4
BR2C1 = 0;
%Qin
BR2C2 = 0;
%Tair
% dT3dt   = -(((khsl*csca)/(mhsl*chsl*lhsl))*(T3 - T4)) +
(((kpet*csca)/(mhsl*chsl*lpet ))*(T2 - T3))
AR3C1 = 0;
%T1
AR3C2 = ((kpet1 *csca)/(mhsl*chsl1*lpet ));
%T2
AR3C3 = -(((khsl1*csca)/(mhsl*chsl1*lhsl))+((kpet1 *csca)/(mhsl*chsl1*lpet
)));%T3
AR3C4 = ((khsl1*csca)/(mhsl*chsl1*lhsl));
%T4
BR3C1 = 0;
%Qin
BR3C2 = 0;
%Tair
```

```
%  dT4dt   = -(((kpvc*csca)/(mpvc*cpvc*lpvc))*(T4-Tair)) +
(((khsl*csca)/(mpvc*cpvc*lhsl)*(T3 - T4)))
%T4
AR4C1 = 0;
%T1
AR4C2 = 0;
%T2
AR4C3 = ((khsl1*csca)/(mpvc*cpvc1*lhsl));
%T3
AR4C4 = -
(((kpvc1*csca)/(mpvc*cpvc1*lpvc))+((khsl1*csca)/(mpvc*cpvc1*lhsl)));%T4
BR4C1 = 0;
%Qin
BR4C2 = ((kpvc1*csca)/(mpvc*cpvc1*lpvc));
%Tair
AA =    [AR1C1,AR1C2,AR1C3,AR1C4;
AR2C1,AR2C2,AR2C3,AR2C4;
AR3C1,AR3C2,AR3C3,AR3C4;
AR4C1,AR4C2,AR4C3,AR4C4;];
BB =    [BR1C1, BR2C2;
BR2C1, BR2C2;
BR3C1, BR3C2;
BR4C1, BR4C2;];
CC =    [1 0 0 0;
0 1 0 0;
0 0 1 0;
0 0 0 1;];
```

```
DD =    [0];
Th = 200; T1 = Tair; T2 = Tair; T3 = Tair; T4 = Tair;
y1 = [T1,T2,T3,T4];
%state space systems
sys1 = ss(AA,BB,CC,DD);
stepSize   = 0.1;
maxTime    = 80;
ttime       = 0:stepSize:maxTime;
[v, q]      = size(ttime);
QQin        = Tair*ones(1,q);
QQQin       = Qin*ones(1,q);
TTair       = Tair*ones(1,q);
ww          = round(lowPercent*q);
vv          = round(highPercent*q);
% Add noise to array
for a = 1:ww-1
QQin(a) = awgn(Tair,20);
end
for b = vv+1:length(ttime)
QQin(b) = awgn(Tair,20);
end
for c = ww:vv
QQin(c) = awgn(Qin,20);
end
for d = 1:maxTime*10
TTair(d) = awgn(Tair,20);
QQQin(d) = awgn(Qin,20);
end
```